

Imaging of Cerebritis, Encephalitis, and Brain Abscess

Tanya J. Rath, MD^{a,*}, Marion Hughes, MD^a,
Mohammad Arabi, MD, FRCR^b, Gaurang V. Shah, MD^b

KEYWORDS

• Central nervous system • Infection • Magnetic resonance imaging

KEY POINTS

- The most common identified sources of brain abscess include: otomastoiditis, sinusitis, odontogenic abscess, hematogenous dissemination from a distant source and neurosurgical complication.
- MRI is sensitive for the detection of brain abscess. Restricted diffusion within a centrally T2 hyperintense ring enhancing mass is characteristic but not pathognomonic of pyogenic brain abscess.
- MRI can demonstrate the complications from brain abscess including intracranial herniation, hydrocephalus, meningitis, subdural or epidural empyema, venous sinus thrombosis and ventriculitis.
- Imaging is critical to the rapid diagnosis of brain abscess, provides guidance for stereotactic localization and is useful for monitoring response following treatment.
- Infectious encephalitis is usually viral in etiology and should be considered in patients complaining of fever and headache with altered level of consciousness or evidence of cerebral dysfunction.
- The MRI features of encephalitis are highly variable according to the offending organism and patient age.
- HSV encephalitis is associated with high mortality and in adults typically causes asymmetric bilateral FLAIR/T2WI hyperintensity in the medial temporal lobes, insular cortex and posterior-inferior frontal lobes with relative sparing of the basal ganglia.

INTRODUCTION

Cerebritis is an area of poorly defined acute inflammation in the brain with increased permeability of the local blood vessels, but without neovascularity or angiogenesis.¹ Cerebritis can result from a variety of etiological factors, including pyogenic infection, and if left untreated in this setting leads to pyogenic brain abscess formation. A pyogenic abscess is a focal area of parenchymal infection that contains a central collection of pus surrounded by a vascularized collagenous capsule.^{1–3} Before the late 1800s brain abscess was typically fatal and only discovered on postmortem examination. In 1893, Sir William Macewen published the

monograph *Pyogenic Infective Diseases of the Brain and Spinal Cord*, which described the successful surgical treatment of 18 of 25 reported intraparenchymal brain abscesses.⁴ Macewen stressed the importance of aseptic surgery, cerebral localization, and early diagnosis as important factors essential to the successful surgical treatment of brain abscess.⁴ After the addition of antibiotic treatment in the early 1940s, mortality from brain abscesses decreased over the next 2 decades but remained high. A multitude of imaging modalities including ventriculography, angiography, and thorotrast administration had a positive impact on the treatment of brain abscess by providing a means to sequentially image the

^a Department of Radiology, University of Pittsburgh Medical Center, 200 Lothrop Street, Presby South Tower, 8th Floor North, Pittsburgh, PA 15213-2582, USA; ^b Department of Radiology, University of Michigan Health System, 1500 East Medical Center Drive, Ann Arbor, MI 48109, USA

* Corresponding author.

E-mail address: rathjt@upmc.edu

abscess cavity.⁵ Since the mid 1970s, mortality from brain abscess has decreased from 30% to 40% to 5% to 20%, with the higher rates reported in developing nations.^{2,6–15} This reduction in mortality has largely been attributed to (1) the advent of commercially available computed tomography (CT) in 1974, and (2) improved targeted antibiotic therapy due to advances in bacteriologic techniques and new antimicrobial agents.^{15–18} CT allows for rapid diagnosis and localization, stereotactic aspiration, and accurate serial postoperative evaluation.^{19,20}

Encephalitis is a diffuse infection or inflammatory process of the brain itself with clinical evidence of brain dysfunction.^{21,22} Infectious encephalitis is typically viral in origin. The diagnosis of viral encephalitis should be strongly considered in patients presenting with febrile disease accompanied by headache, altered level of consciousness, and evidence of cerebral dysfunction. Imaging plays a role in the diagnosis of encephalitis when combined with the medical history, physical examination, serologic studies, and cerebrospinal fluid (CSF) analysis. In addition, there are multiple nonviral causes of infectious encephalitis including bacterial, fungal, parasitic, and rickettsial origins.²¹ The imaging appearances of several common and select uncommon infectious encephalitides along with causes of encephalitis in the pediatric patient population are reviewed in this article. Common causes of encephalitis in immunocompromised patients, and their imaging appearances, are also discussed in this article.

PYOGENIC INFECTION

Pathophysiology

Brain abscess is often categorized by the source of infection, which influences the location of the abscess and the offending organism. The most common identified causes of brain abscess include direct spread from local infections, hematogenous dissemination from a distant source, trauma, and neurosurgical complication. Up to 30% of brain abscesses are reported as cryptogenic.^{2,3,12} Otomastoiditis, sinusitis, and odontogenic abscess are the primary sources of direct spread, which occurs through involvement of bone or via transmission of bacteria to the brain through the valveless emissary veins.³ Otomastoiditis causes abscess formation in the adjacent temporal lobe and cerebellum (**Figs. 1** and **2**). Frontal and ethmoid sinusitis and odontogenic infection are frequently associated with formation of frontal lobe abscess.²³

Abscesses secondary to hematogenous seeding from a distant source are more typically

multiple, near the gray-white junction, and usually in the distribution of the middle cerebral artery.²³ Sources of hematogenous dissemination are variable. Identifying the source of infection is a crucial factor for adequate treatment to prevent recurrent disease. In children, there should be a high index of suspicion for congenital cyanotic heart disease.^{2,24} Examples of other sources include pulmonary abscess, pulmonary arteriovenous malformation (AVM), bacterial endocarditis, and intra-abdominal infections. Dental abscess can result in bacteremia with hematogenous dissemination or local thrombophlebitis.

The epidemiologic trends of brain abscess are changing. Brain abscess is uniformly more common among males than females for unknown reasons, and most commonly occurs during the first 4 decades of life, although all age groups may be affected.¹² Aggressive medical and surgical management of otitis media has led to a decrease in otogenic-related brain abscess in developed countries, although it remains the principal source of brain abscess in developing countries such as India and China.^{9,12} Similarly, there are reports of decreased incidence of brain abscess secondary to congenital cyanotic heart disease in developed countries, likely attributable to earlier and improved surgical repair.⁹ Brain abscess secondary to trauma and neurosurgery has increased.^{9,12,13,25–27} The rising incidence of postsurgical abscess has largely been attributed to the increased volume of neurosurgeries performed (**Fig. 3**). Additional predisposing factors include diabetes mellitus, alcoholism, intravenous drug abuse, pulmonary AVM, and immunosuppression.^{9,13,14}

Clinical Presentation

Symptoms depend on the location of the abscess, degree of mass effect, and associated complications. Headache is the most frequent symptom. Additional symptoms include fever, focal neurologic deficit, nausea, vomiting, and seizure. Laboratory tests add little to the diagnosis. The white blood cell count is variably elevated and the absence of a leukocytosis does not exclude the diagnosis.^{2,11,13,14} Lumbar puncture may be contraindicated because of mass effect and elevated intracranial pressure. CSF analysis can be normal, and when abnormal typically demonstrates a nonspecific elevation in protein and white blood cells that does not aid in diagnosis or treatment. In the absence of intraventricular rupture, CSF cultures are frequently sterile.^{2,11,14} In cases of hematogenous dissemination blood cultures should be performed, as they may identify the causative organism.

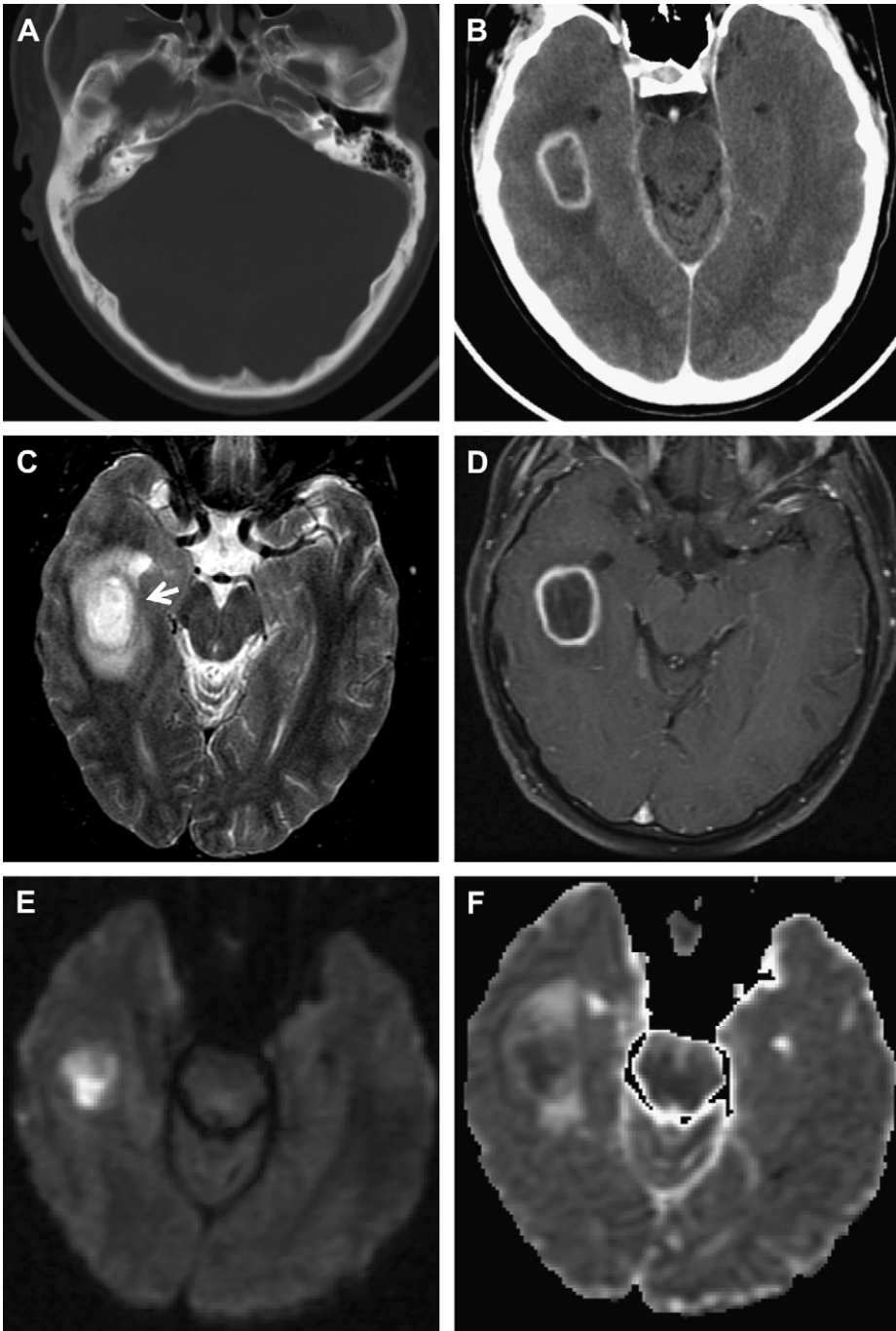


Fig. 1. A patient who presented with ear infection and headache. (A) CT bone window demonstrates complete opacification of the right middle ear cleft and poorly pneumatized right mastoid, consistent with chronic right otomastoiditis. (B) On contrast-enhanced CT there is an associated ovoid ring-enhancing mass in the right temporal lobe with surrounding vasogenic edema. (C) On axial T2-weighted sequence, it has central hyperintense signal corresponding to the pus cavity and the characteristic surrounding T2 hypointense signal of the abscess capsule (*white arrow*). Local mass effect results in entrapment of the adjacent mildly dilated right temporal horn. (D) Axial T1 postcontrast sequence demonstrates typical smooth ring enhancement of a mature abscess. (E, F) Corresponding diffusion-weighted sequence and apparent diffusion coefficient (ADC) maps confirm restricted diffusion within the abscess cavity.

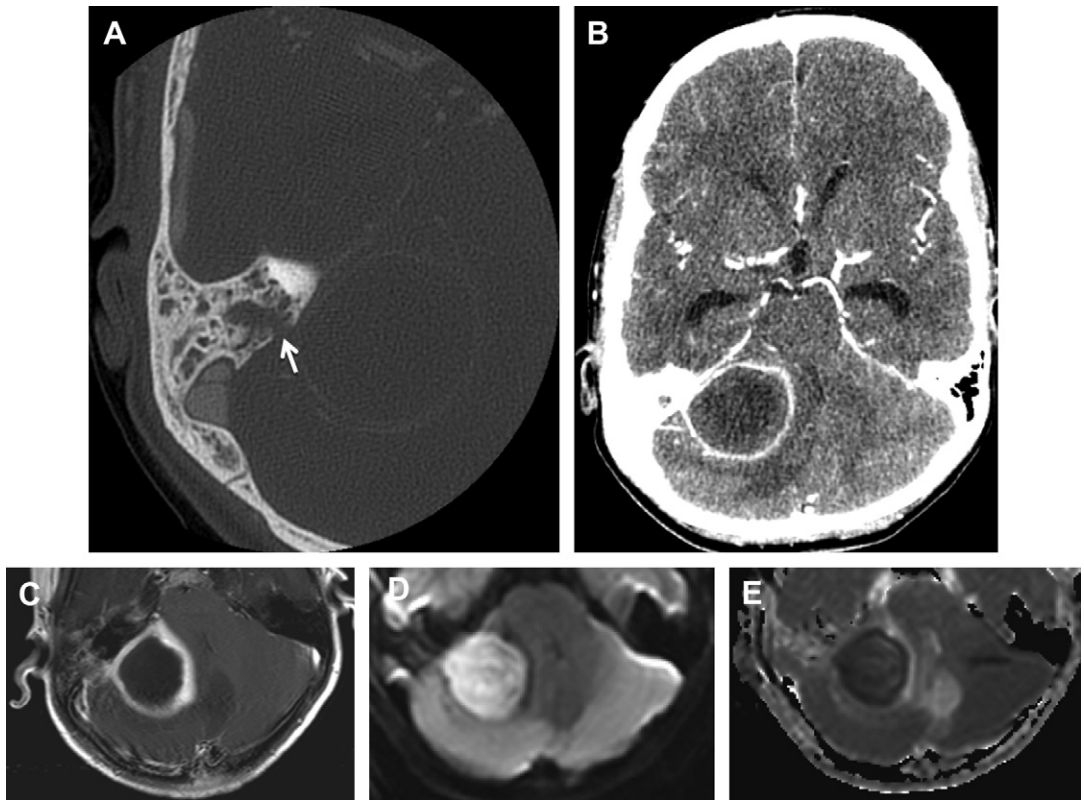


Fig. 2. A patient who presented with complaints of earache and fever. (A) Temporal bone CT demonstrates mastoiditis with opacification of the right mastoid air cells and bone dehiscence along the dorsal right petrous temporal bone (*white arrow*). An adjacent ring-enhancing mass is seen in the right posterior fossa. (B) Contrast-enhanced head CT confirms an adjacent round smooth rim-enhancing abscess in the right cerebellar hemisphere. Mass effect displaces the fourth ventricle to the left, and there is associated hydrocephalus. (C) On axial T1-weighted postcontrast MR imaging the abscess demonstrates a ring of enhancement with central T1 hypointense signal. (D) Diffusion-weighted sequence demonstrates central hyperintense signal. (E) On the corresponding ADC map there is central hypointense signal, confirming restricted diffusion in the abscess cavity. (Courtesy of Hemant Parmar, MD, University of Michigan.)

The offending microbes vary with the source of infection and frequently are polymicrobial. The most common implicated organisms include microaerophilic streptococci, anaerobic bacteria, *Staphylococcus aureus*, and facultative gram-negative bacteria.^{2,3,9,11–14,26} In particular, nocardia brain abscess is reportedly difficult to treat and has been associated with high mortality.²⁸ Ideally antibiotic therapy should be targeted based on culture results from aspiration.

Radiologic Imaging

Progressing from cerebritis to abscess formation, the imaging characteristics change depending on the time of imaging. Britt and Enzmann²⁹ described the spectrum in 4 separate stages including early cerebritis, late cerebritis, early capsule formation, and late capsule formation,

based on observed gross surgical, histopathologic, and CT criteria. During the early cerebritis phase, bacteria arrive to the brain parenchyma, and there is an inflammatory response that grossly results in softening of the brain and histopathologically corresponds to perivascular inflammatory cuffing poorly delineated from surrounding normal brain. On noncontrast CT, this corresponds to an area of ill-defined low attenuation with a variable pattern of contrast enhancement ranging from no enhancement to nodular or ringlike enhancement. The enhancement pattern is unchanged or progresses on delayed images obtained at 30 to 60 minutes after contrast administration. During the late cerebritis phase, pathologically there is progression of central necrosis, and fibroblasts deposit an early reticulin matrix around the periphery. On noncontrast CT there is persistent poorly defined low-attenuation edema; however,

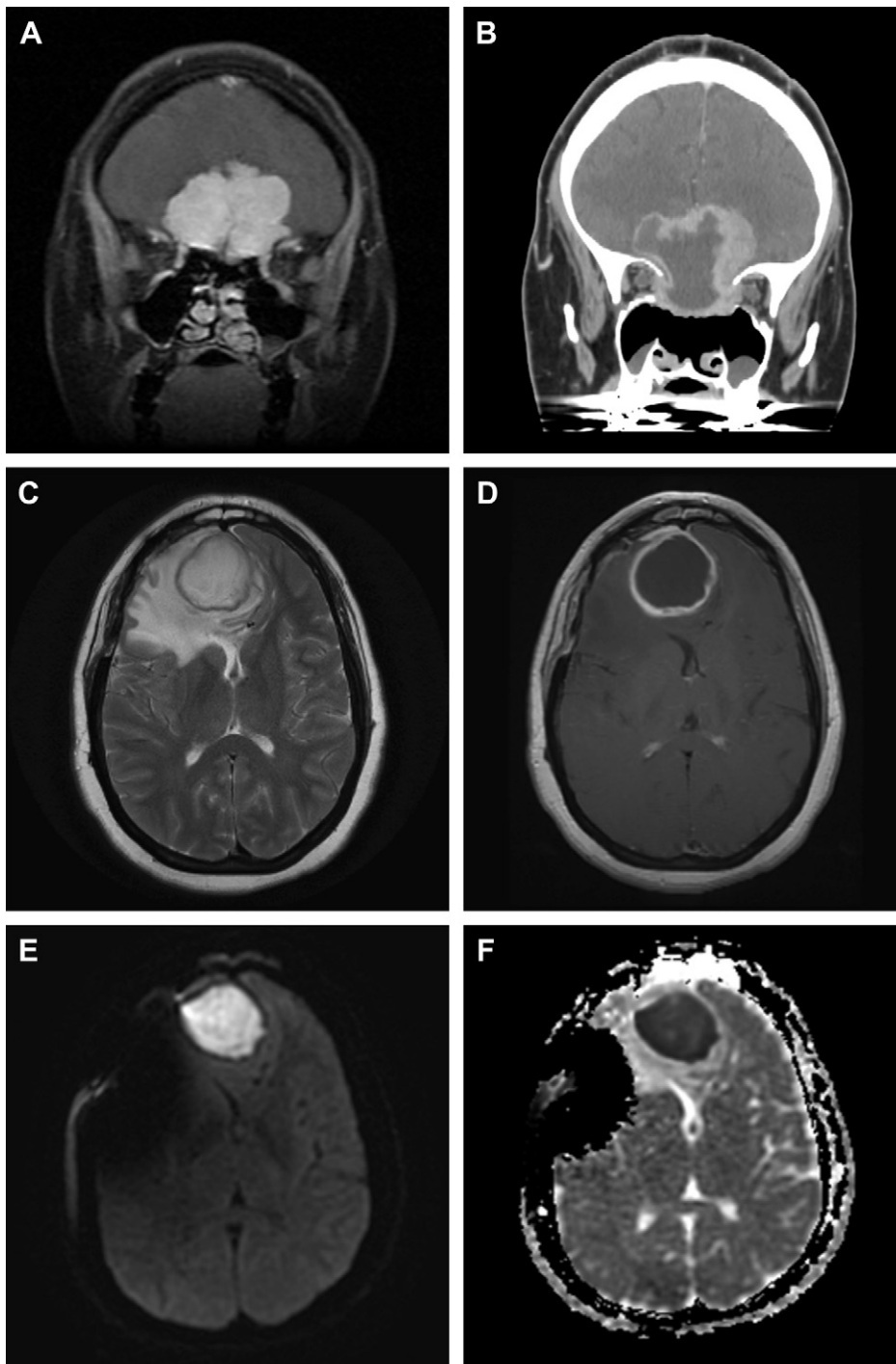


Fig. 3. A 36-year-old woman with a history of headaches. (A) Coronal T1 postcontrast fat-saturated sequence demonstrates an enhancing extra-axial mass along the floor of the anterior cranial fossa, characteristic of an olfactory groove meningioma. (B) Reconstructed coronal CT postcontrast image demonstrates partial resection of the mass that was done via a staged expanded endonasal and subfrontal approach. Postoperative course was complicated by recurrent frontal sinusitis and CSF leak requiring surgical repair. (C, D) Axial T2 and T1 post-contrast images demonstrate a large right frontal abscess with a characteristic T2 hypointense enhancing capsule. There is extensive surrounding vasogenic edema and mass effect displacing the anterior falx cerebri toward the left. There is associated opacification of the frontal sinus related to chronic sinusitis. (E, F) Hyperintense signal on the diffusion-weighted image and hypointense signal on the ADC map within the mass are consistent with restricted diffusion and typical of pyogenic abscess. Cultures from the abscess grew *Streptococcus milleri*. Susceptibility artifact in the right frontal region is from surgical hardware.

on postcontrast images there is thick ringlike or nodular enhancement that is stable or increases on delayed images. During the early and late capsule stage, there is a central core containing pus that may be round, oval, or multiloculated, with a surrounding capsule. The capsule consists of a reticulin network with scant collagen during the early stage, and progresses to a mature collagen capsule with a zone of surrounding gliosis during the late stage. On noncontrast CT during both the early and late capsule stages, the pus-containing core appears as a round or ovoid area of low attenuation with a sometimes faintly visible surrounding capsule ring. Following contrast administration, there is ring enhancement that decays on delayed images corresponding to the granulation tissue of the capsule. The medial or ventricular wall of the abscess cavity may be thinner than the lateral wall, attributed to differences in capsule blood supply. It is more prone to rupture and can lead to daughter abscess formation.

Magnetic resonance (MR) imaging is more sensitive than CT in the detection of brain abscess because it has greater sensitivity to changes in tissue water content, resulting in greater contrast between edematous brain and normal brain during the early stages of cerebritis and abscess formation.³⁰ During the early cerebritis stage, there is nonspecific poorly defined hyperintensity on T2-weighted sequence that is isointense to mildly hypointense on T1-weighted images, with ill-defined enhancement (Fig. 4).³¹ The characteristic MR imaging features of the necrotic center of a mature brain abscess include fluid hyperintense relative to CSF and hypointense relative to white

matter on the T1-weighted sequence. On T2-weighted sequences, the fluid in the abscess cavity is iso- to hyperintense to CSF and gray matter. This characteristic pattern of T2 prolongation relative to normal brain and T1 shortening relative to CSF reflects the proteinaceous nature of the abscess fluid.³⁰ Vasogenic edema surrounding the abscess cavity is characterized by surrounding hypointensity on the T1-weighted sequence and hyperintensity on the T2-weighted sequence. Interposed between the abscess cavity and the surrounding vasogenic edema is the abscess capsule, which is a smooth, circumferential ring that is iso- to hyperintense to white matter on the T1 sequence, iso- to hypointense on the T2-weighted sequence, and enhances on postcontrast images. The unique hypointensity of the capsule relative to white matter on T2-weighted sequences has been attributed to T1 and T2 shortening, occurring as a result of free radicals generated by phagocytic macrophages entering the capsule wall.³⁰

The pathologic and imaging features of pyogenic abscess formation reflects the attempt by the host's immune system at containing the infection in immunocompetent patients. Experimental brain abscess models in immunocompetent mice indicate that microglia and astrocytes release chemokines and cytokines that result in an inflammatory response aimed at containing and eradicating the infection.³¹ In immunocompromised patients with an impaired inflammatory response, there may be a lack of ring enhancement and less vasogenic edema in comparison with immunocompetent patients, features considered to be a poor prognostic finding.^{32,33}

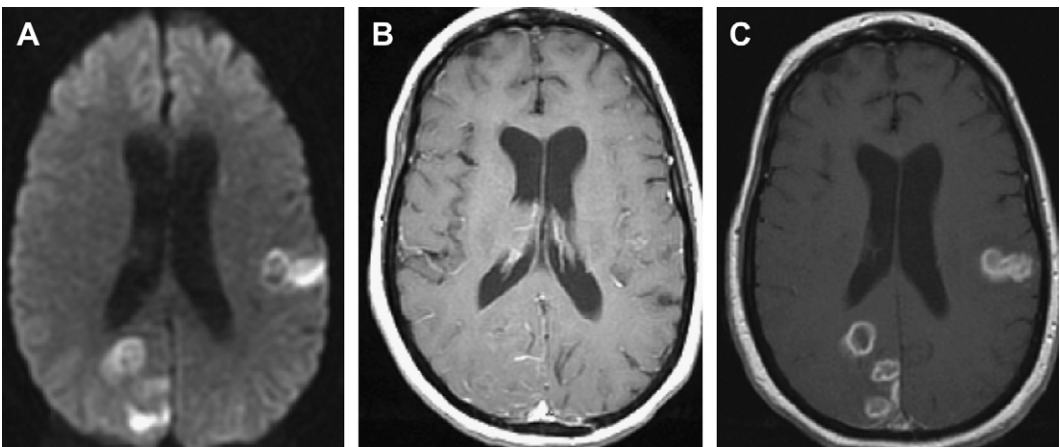


Fig. 4. Progression from cerebritis to abscess. (A, B) Axial diffusion-weighted sequence and T1 postcontrast image demonstrate areas of restricted diffusion in the left temporal lobe and the posterior right cerebral hemisphere that demonstrate some poorly defined enhancement. (C) Follow-up axial T1 postcontrast sequence 7 days later demonstrates progression to rim enhancement typical of abscess formation. (Courtesy of Hemant Parmar, MD, University of Michigan.)

Complicating factors that may be present on imaging include local mass effect with intracranial herniation, hydrocephalus, meningitis, and extra-axial fluid collection (Figs. 5 and 6). Local thrombophlebitis can result in venous sinus thrombosis. Intraventricular rupture with ventriculitis is a devastating complication associated with high mortality, and appears as ventricular debris and abnormal ependymal enhancement (Figs. 7 and 8).³⁴

The classic ring-enhancing appearance of a capsule stage abscess on CT and conventional MR imaging is, however, nonspecific, and the differential diagnosis includes nonpyogenic abscess, high-grade primary central nervous system (CNS) neoplasm, metastasis, infarct, hematoma, thrombosed giant aneurysm, radiation necrosis, and demyelinating disease. Immunocompromised patients deserve special consideration because they are uniquely susceptible to a variety of opportunistic infections and neoplastic processes. *Toxoplasmosis gondii* infection, primary CNS lymphoma, and nonpyogenic abscesses should also be considered in these patients. Clinical data may be helpful in narrowing the differential of a ring-enhancing intraparenchymal brain mass, but is frequently of limited value in differentiating abscess from metastases or high-grade glioma because of the unreliable presence of infectious signs in the setting of abscess. Imaging features favoring abscess include (1) 2- to 7-mm continuous smooth, thin rim of enhancement, (2) T2 hypointense rim, and (3) thinning along the medial wall. However, these features are not consistently present and none are 100% specific.^{1,30,35} Consequently, attempts have been made to differentiate ring-enhancing neoplasm from brain abscess using additional noninvasive imaging techniques.

Nuclear medicine has a limited role in the evaluation of brain abscess. Brain abscesses are usually localized by MR imaging or CT because patients present with headache or other neurologic signs. Some investigators report that the use of the oncotropic tracer thallium-201 chloride in conjunction with MR imaging or CT improves diagnostic confidence in distinguishing abscess from neoplasm.³⁶ However, this application has not been reliable and there are reports of false-positive thallium-201 chloride uptake in brain abscesses.³⁷ Its main application has been in distinguishing CNS lymphoma from *T gondii* infection in human immunodeficiency virus (HIV)-positive patients, with sensitivity of 92% and specificity of 89% for the diagnosis of CNS lymphoma.³⁸

Diffusion-weighted imaging is helpful in distinguishing ring-enhancing neoplasm from pyogenic abscess. The central nonenhancing portion of a ring-enhancing neoplasm usually demonstrates

facilitated diffusion while restricted diffusion within a ring-enhancing mass is characteristic, but not pathognomonic, of a brain abscess.^{35,39–42} It appears as a central bright signal on the diffusion-weighted sequence and reduced apparent diffusion coefficient (ADC) values on the ADC map. Whereas some investigators attribute the restriction of water proton mobility within the abscess cavity to necrotic debris, macromolecules, and viscosity of pus, in vivo and ex vivo studies by Mishra and colleagues^{35,39,43} suggest viable bacteria and inflammatory cells in the abscess cavity primarily account for the restricted diffusion. Furthermore, there are reports of higher ADCs in treated abscesses, as well as some data to suggest that persistent low ADC or recurrent low ADC in an abscess cavity following treatment indicates reactivation of infection or failed therapy.^{44,45} Infrequently there is overlap of the diffusion-weighted imaging features of neoplasm and abscess, with some aseptic ring-enhancing neoplasms demonstrating restricted diffusion and some reports of facilitated diffusion within pyogenic abscess cavities, typically when empiric antibiotic therapy has preceded imaging.^{46–51} The reported sensitivity and specificity of diffusion-weighted imaging in differentiating abscess from other pathology ranges from 72% to 95% and from 96% to 100%, respectively.^{43,48}

Advanced Imaging

In vivo ¹H nuclear MR (¹H-NMR) spectroscopy complements diffusion-weighted imaging and conventional MR imaging. ¹H-NMR can improve diagnostic confidence in distinguishing cystic or necrotic tumor from abscess.⁴⁸ In the late capsule stage, bacterial abscesses have necrotic centers that lack the normal brain metabolites of *N*-acetylaspartate (NAA), choline, and creatine. Elevated levels of cytosolic amino acids (0.9 ppm) and lactate (1.3 ppm) with or without acetate (1.9 ppm) and succinate (2.4 ppm) are the characteristic resonances within the cavity of untreated pyogenic abscess.^{52–54} While lactate and lipid signal can be found in the in vivo ¹H-NMR spectra of both brain tumor and abscess, cytosolic amino acids (valine, leucine, and isoleucine) are a key marker of pyogenic abscess which, when present, suggest its diagnosis (Fig. 9). These amino acids are not detectable on in vivo ¹H-NMR spectra from cystic or necrotic brain tumors.⁵⁵ The increased levels of lactate, acetate, and succinate are the by-product of glycolysis and fermentation by the causative bacteria. The amino acids are a result of proteolysis by polymorphonucleocytes in pus.^{51,53} Acetate, with or without succinate, is not typically present

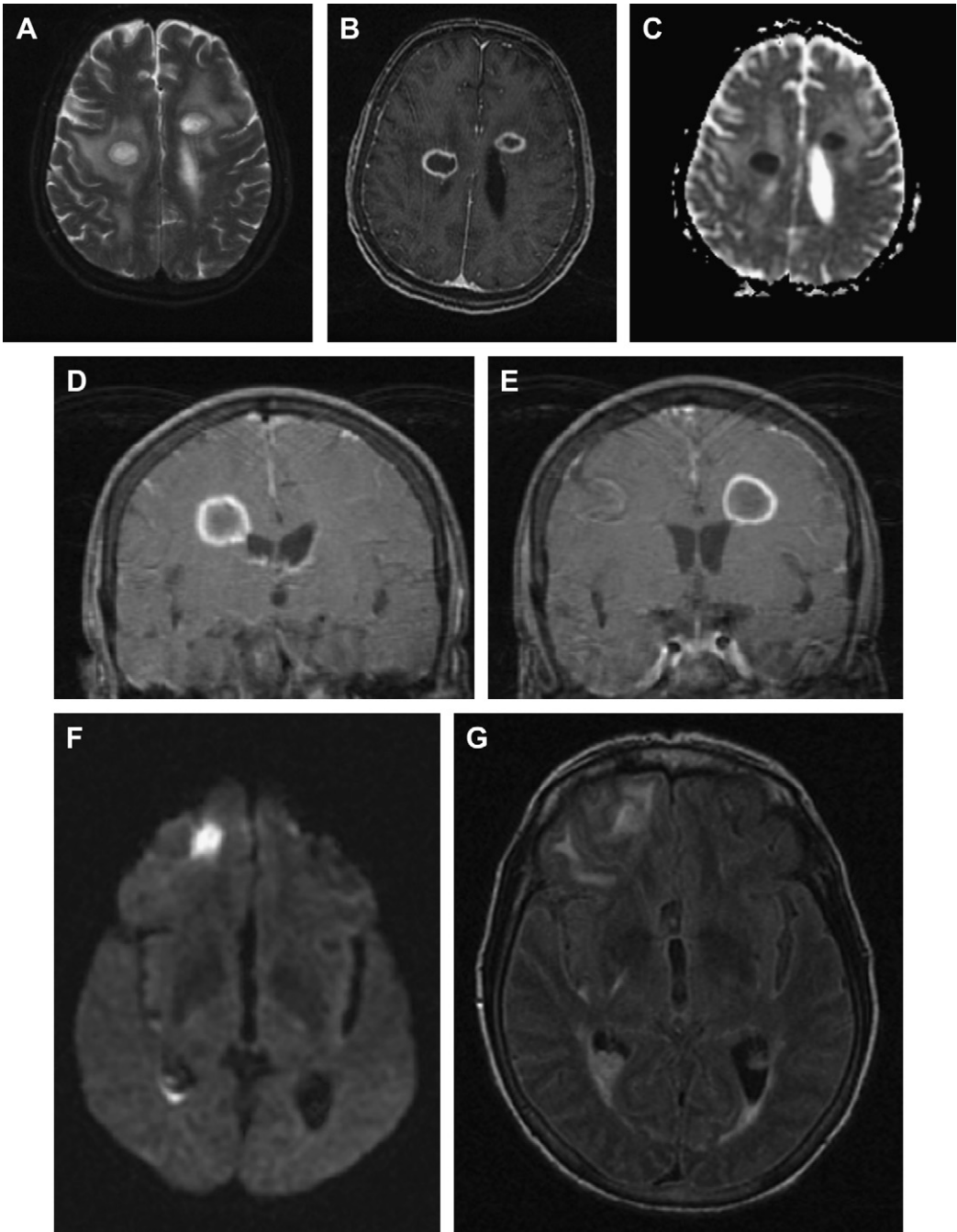


Fig. 5. A 68-year-old woman presented with altered mental status. (A–C) T2, T1 postcontrast, and ADC maps demonstrate multiple bilateral abscesses with central T2 hyperintense signal and surrounding T2 hypointense signal, peripheral smooth rim enhancement, and reduced ADC values. There is characteristic thinning of the capsules along the ventricular margins. (D, E) Coronal T1 postcontrast images redemonstrate thinning along the medial margin of the abscess capsules where they communicate with the ventricular system. There is associated abnormal ependymal enhancement (*white arrow*). (F, G) Diffusion-weighted sequence and fluid-attenuated inversion recovery (FLAIR) sequence confirm intraventricular rupture and ventriculitis, with debris layering dependently in the ventricular system. (Courtesy of William Delfyett, MD, University of Pittsburgh.)

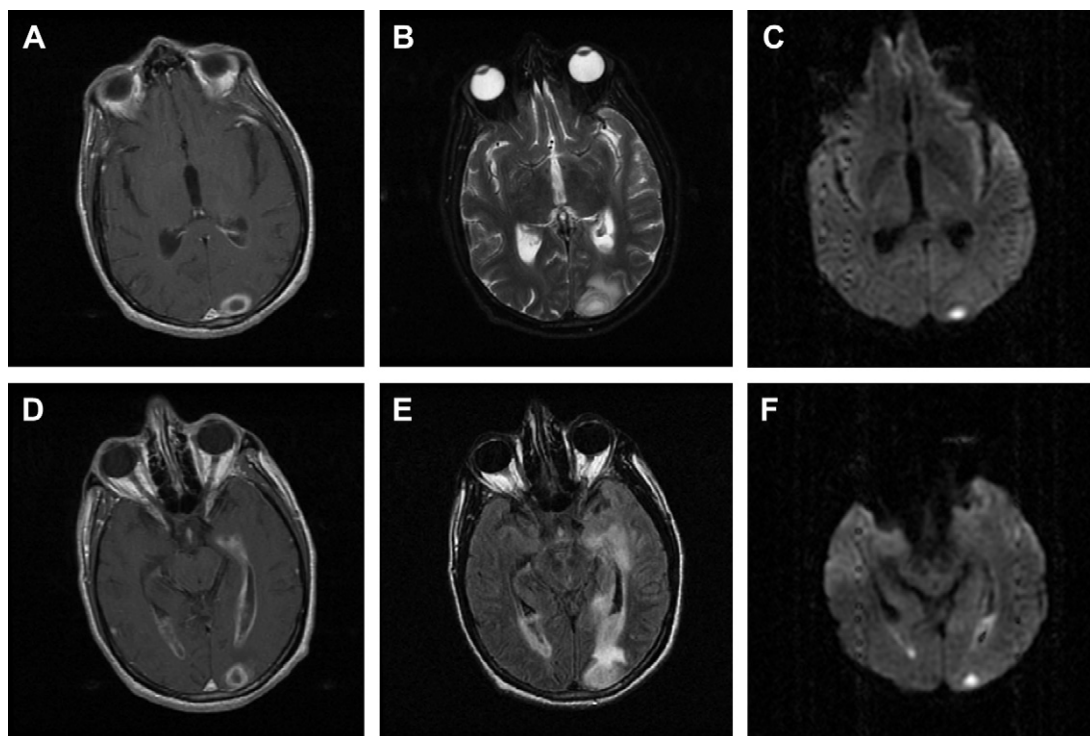


Fig. 6. A 57-year-old male alcoholic who presented with altered mental status. (A–C) Axial T1 postcontrast, T2, and diffusion-weighted sequences demonstrate a characteristic left occipital abscess with rim enhancement, central T2 hyperintensity, and bright signal on the diffusion-weighted sequence, which was confirmed to represent true restricted diffusion by ADC maps. There is surrounding mild vasogenic edema. (D–F) Axial T1 postcontrast, FLAIR, and diffusion-weighted sequences demonstrate associated intraventricular rupture with ventriculitis as demonstrated by abnormal ependymal enhancement, and layering debris in the ventricular system that restricts diffusion. (Courtesy of William Delfyett, MD, University of Pittsburgh.)

in brain abscesses caused by aerobic infection, but has been reported in abscesses caused by anaerobic and facultative anaerobic microorganisms.^{54,56} Following treatment, the resonances of amino acids have been reported to disappear.^{41,48,51,57} The reported sensitivity and specificity of MR spectroscopy in distinguishing abscess from other pathology is 72% to 96% and 30% to 100%, respectively.^{48,50,54–56}

There are few published articles on the role of perfusion imaging in distinguishing brain abscess from necrotic or cystic ring-enhancing neoplasms. In a recent prospective study, Chiang and colleagues found that the mean relative cerebral blood volume of brain tumor walls was statistically significantly higher than that of cerebral abscesses. This difference was attributed to a greater degree of vascularity and blood-brain barrier breakdown in the wall of neoplasm versus the collagenous wall of a mature abscess.^{58,59}

Recent research has focused on the microstructure of the abscess cavity using diffusion tensor

imaging (DTI). Elevated DTI-derived fractional anisotropy within brain abscess cavities has been demonstrated, and has a positive correlation with neuroinflammatory molecules in pus.^{60,61} Similarly, a positive correlation between fractional anisotropy in heat-killed *S aureus*-treated cell lines has been demonstrated.⁶¹ These findings support the hypothesis that increased fractional anisotropy is due to upregulation of neuroinflammatory adhesion molecules, causing a structured orientation of inflammatory cells in the abscess cavity. In a small study, Nath and colleagues⁵¹ found that increased fractional anisotropy and reduced mean diffusivity had 100% and 75% sensitivity, respectively, in predicting pyogenic abscess. Furthermore, fractional anisotropy in abscess cavities has been shown to decrease following treatment while mean diffusivity did not significantly change, suggesting that in the future, surveillance of fractional anisotropy may serve as a marker of inflammation and could help to guide therapy, although additional research is required.⁶²

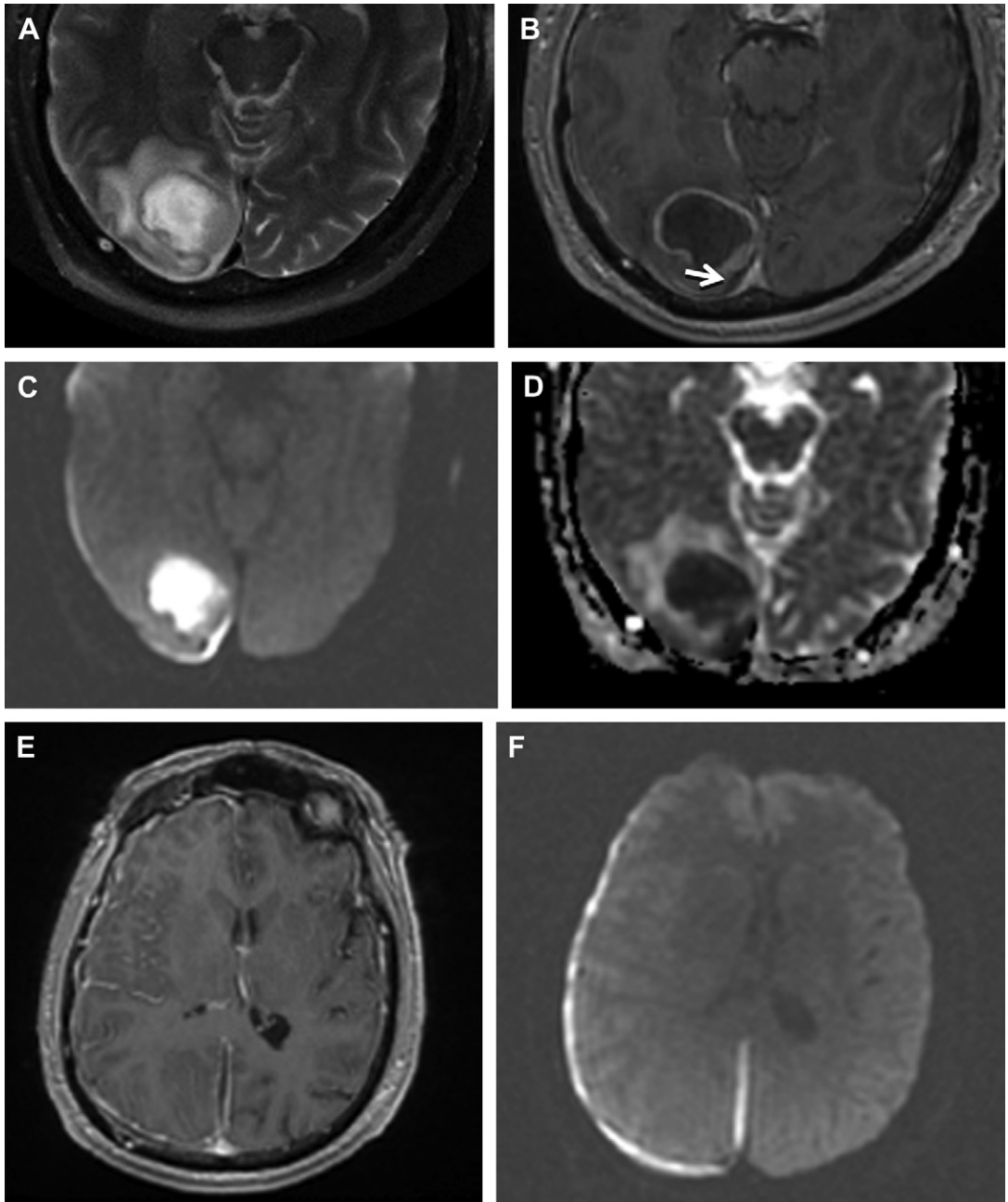


Fig. 7. (A, B) A T2 hyperintense right occipital abscess demonstrates central T2 hyperintense signal in the abscess cavity, T2 hypointense signal in the capsule, and capsule rim enhancement. There is surrounding vasogenic edema. There is an adjacent small subdural empyema medial to the abscess (*white arrow*). (C, D) Axial diffusion-weighted sequence and ADC map confirm restricted diffusion in the abscess cavity and within the small right tentorium subdural empyema. (E) On axial T1 postcontrast sequence there is a rim-enhancing subdural fluid collection extending over the right cerebral convexity and along the right posterior falx cerebri. There is associated mild local mass effect and meningitis with leptomenigeal enhancement over the right cerebral hemisphere (F). On the diffusion-weighted sequence the subdural fluid collection demonstrates restricted diffusion, consistent with an associated subdural empyema.

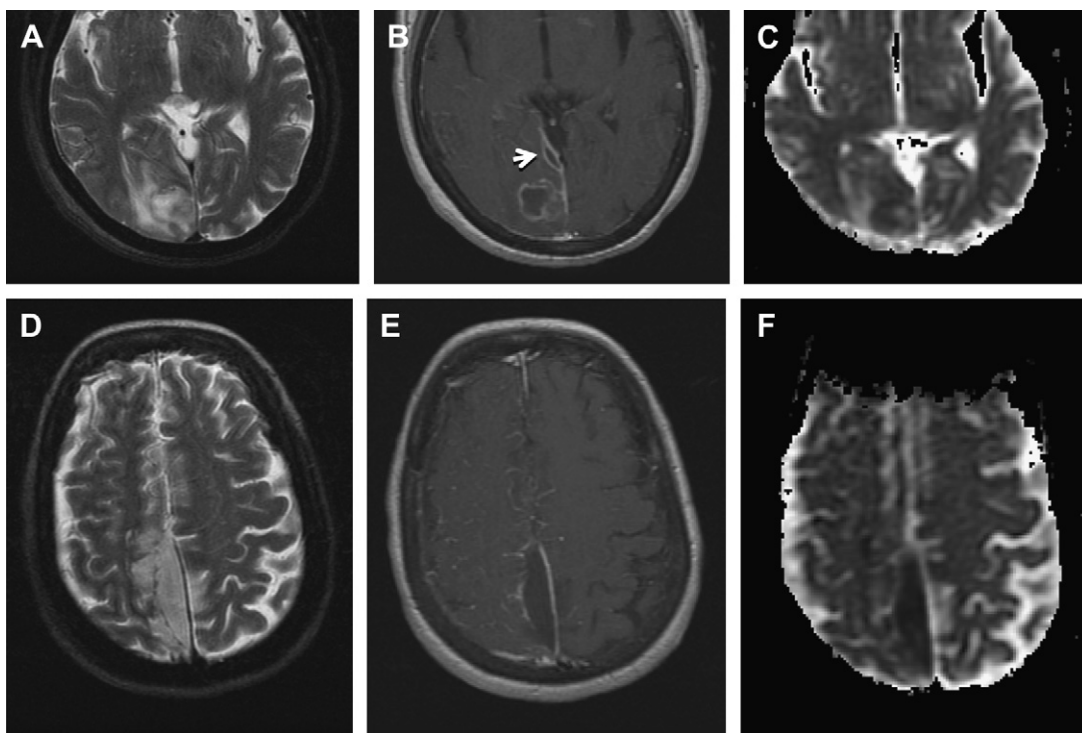


Fig. 8. (A–C) Axial T2-weighted sequence, T1 postcontrast sequence, and ADC maps demonstrate a typical brain abscess in the right occipital lobe with central T2 hyperintense signal, surrounding rim enhancement, and hypointense signal on ADC, consistent with restricted diffusion. There is daughter abscess formation beginning along its medial margin. There is a rim-enhancing small subdural empyema along the right tentorium (*white arrow*). (D–F) There is an associated right posterior parafalcine T2 hyperintense rim-enhancing subdural fluid collection with reduced ADC, consistent with a subdural empyema. In addition, there is evidence of meningitis with leptomenigeal enhancement noted in the right cerebral hemisphere. (Courtesy of Barton F. Branstetter IV, MD, University of Pittsburgh.)

Treatment

Cerebritis is typically treated with high-dose intravenous antibiotics alone and serial imaging to ensure response to therapy.⁶³ Brain abscesses larger than 2.5 cm or associated with mass effect are usually treated with stereotactic aspiration or excision combined with intravenous antibiotics. Antibiotic therapy is continued for 6 to 8 weeks with serial imaging weekly or biweekly, depending on the patient's clinical condition.^{2,63} Patients who are poor surgical candidates, have numerous small abscesses or have surgically inaccessible disease may be treated with intravenous antibiotics alone. However, diagnostic aspiration should be performed when possible to optimize targeted antibiotic therapy. Unfavorable outcomes have been associated with the presence of an underlying medical condition, sepsis, nocardia abscess, poor neurologic status at presentation, and intraventricular rupture.^{9,12,14,25,28,64,65}

ENCEPHALITIDES

Herpes Simplex Encephalitis

Herpes simplex encephalitis (HSE) is the most common cause of sporadic fatal encephalitis in the United States, with approximately 2000 cases per year.^{21,66} HSE results in necrotizing encephalitis.⁶⁷ About 90% of the cases of HSE are caused by herpes simplex virus type 1 (HSV-1) with approximately 10% of cases being caused by HSV-2; the latter typically is seen in neonates, and is discussed in the pediatrics article by Parmar and colleagues elsewhere in this issue.²¹ Patients with HSE typically present with headache, fever, seizures, viral prodrome, and mental status changes. The classic imaging findings are bilateral asymmetric involvement of the temporal and inferior frontal lobes with less common involvement of the insula and cingulate gyri.⁶⁸ The involved brain typically demonstrates high signal on T2-weighted images and gyral expansion. Fluid-attenuated

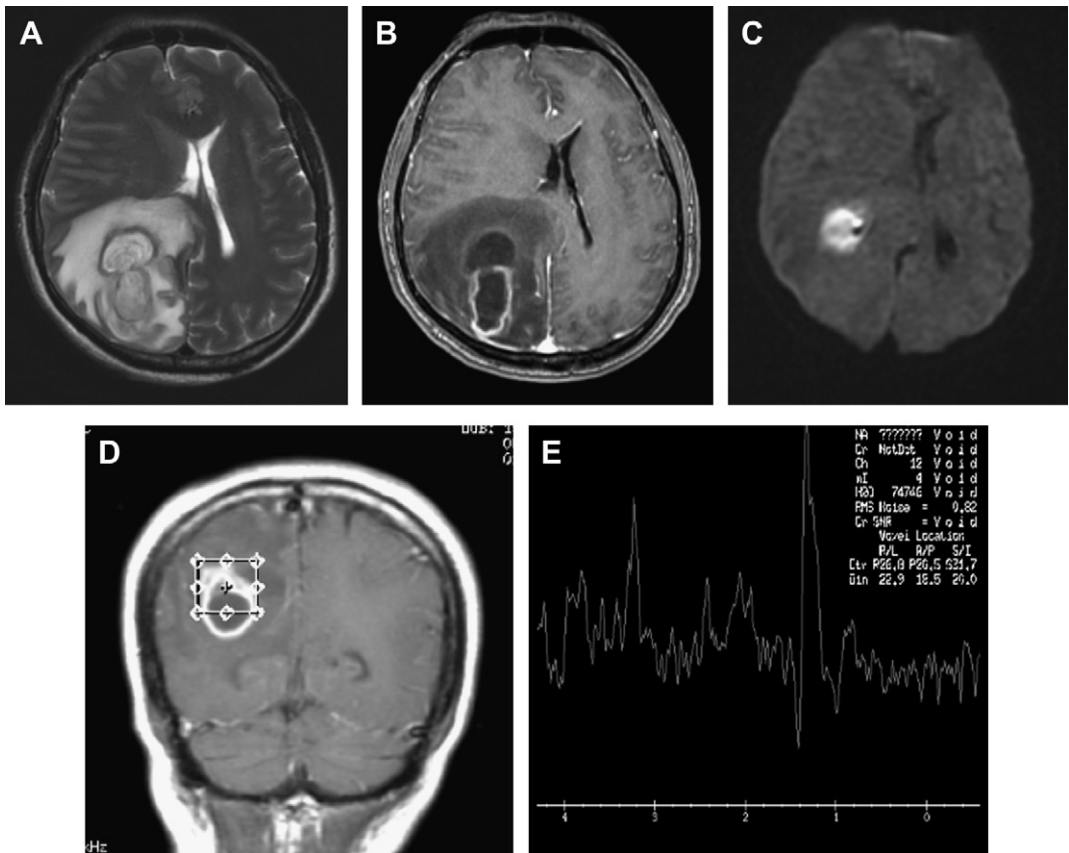


Fig. 9. A patient with a history of intravenous drug abuse who complained of drowsiness, headache, and left hemiparesis. (A–C) Axial T2, T1 postcontrast, and diffusion-weighted images demonstrate a bilobed cystic mass in the right parietal lobe with some surrounding T2 hypointense signal, rim enhancement, and restricted diffusion typical of an abscess in the anterior cystic portion. (D, E) Single-voxel, 144 millisecond echo time, proton MR spectroscopy supports the diagnosis of brain abscess, showing a prominent lipid and smaller inverted lactate peak at 1.3 ppm, amino acids at 0.9 ppm, acetate at 1.9 ppm, and presence of succinate at 2.4 ppm. Mildly elevated choline is also noted at 3.2 ppm. (Courtesy of Suyash Mohan, MD, Penn State University.)

inversion recovery (FLAIR)/T2-weighted sequences demonstrate increased signal in both the swollen cortex and subcortical white matter. Restricted diffusion and petechial hemorrhages may be seen. Gyriiform enhancement may be noted, but is typically a later finding.^{68,69} The basal ganglia are rarely involved in HSE, which helps to distinguish this disease process from other encephalitides.⁶⁸ Thus when insular and subinsular involvement is noted but the signal abnormality abruptly stops at the lateral putamen, HSE should be considered (Fig. 10). Corresponding CT findings include areas of hypoattenuation and gray-white differentiation loss. Metabolic alterations have been demonstrated by MR spectroscopy in cases of HSE with reduced NAA, elevated choline compounds, and sometimes elevated lactate.^{70–72} However, the role of MR spectroscopy in the diagnosis of HSE is limited, as treatment is typically initiated when there is clinical

suspicion and corresponding imaging findings are consistent with HSE. Acyclovir is the treatment of choice for HSE (Class IA evidence).²² Furthermore, treatment with acyclovir for HSE should be immediately begun when there is clinical suspicion of HSE, as mortality rates in untreated HSE are approximately 70%; early initiation of acyclovir decreases mortality to 20% to 30%.²²

HSV-2, the genital strain, causes infections typically in the neonatal period, and is thought to be transmitted to the fetus transplacentally or to the neonate during delivery from a mother with genital herpes. HSV-2 is covered in the pediatrics article in this issue.

Varicella Zoster Virus

Primary varicella zoster virus (VZV) infection typically occurs in children and is known as

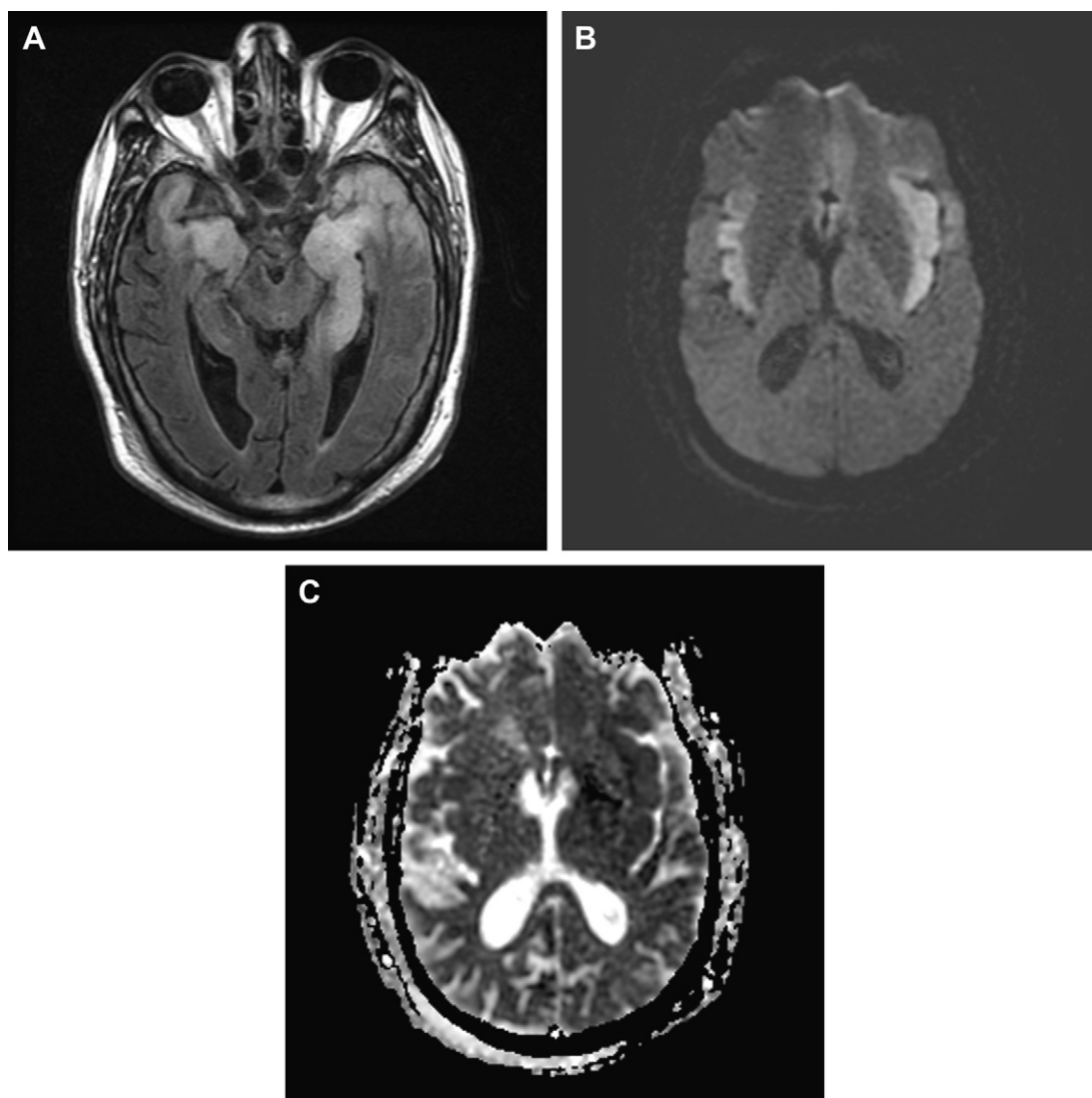


Fig. 10. Herpes simplex encephalitis. Axial FLAIR (A) image demonstrates bilateral, asymmetric temporal lobe signal abnormalities. Diffusion-weighted image (B) and the corresponding ADC map (C) demonstrate areas of restricted diffusion. Postcontrast T1 images (not shown) demonstrated minimal associated enhancement.

chickenpox or varicella. Subsequently the virus becomes latent in ganglionic neurons along the neuroaxis.⁷³ VZV can reactivate in patients, typically in elderly individuals whose cell-mediated immunity to VZV has declined or in immunosuppressed patients. When VZV reactivates the result is zoster or shingles, a painful rash that is caused when the virus travels along the sensory nerve from the dorsal root ganglion to the skin. Zoster is frequently followed by chronic pain known as post-herpetic neuralgia.⁷³ However, other sequela of VZV infection include vasculopathy, myelopathy, retinal necrosis, and cerebellitis. Of note, the CNS complications of VZV reactivation can occur in the absence of a rash.⁷³ VZV infection

has frequently been described as a meningoencephalitis and vasculopathy, but the vasculopathy is thought to be the dominant component.⁷³ Typically both large-vessel and small-vessel arteries are involved, although involvement of either small or large arteries alone can be seen (Fig. 11).^{73,74} The infection is primarily in the media of the arteries.⁷³ Patients often present with an acute stroke or transient ischemic attacks; additional common clinical presentations include headache, cranial neuropathies, changes in mental status, aphasia, ataxia, hemisensory loss, and vision loss. The imaging appearance is of multiple areas of high signal on the T2-weighted image, classically involving the gray-white junction, with purely

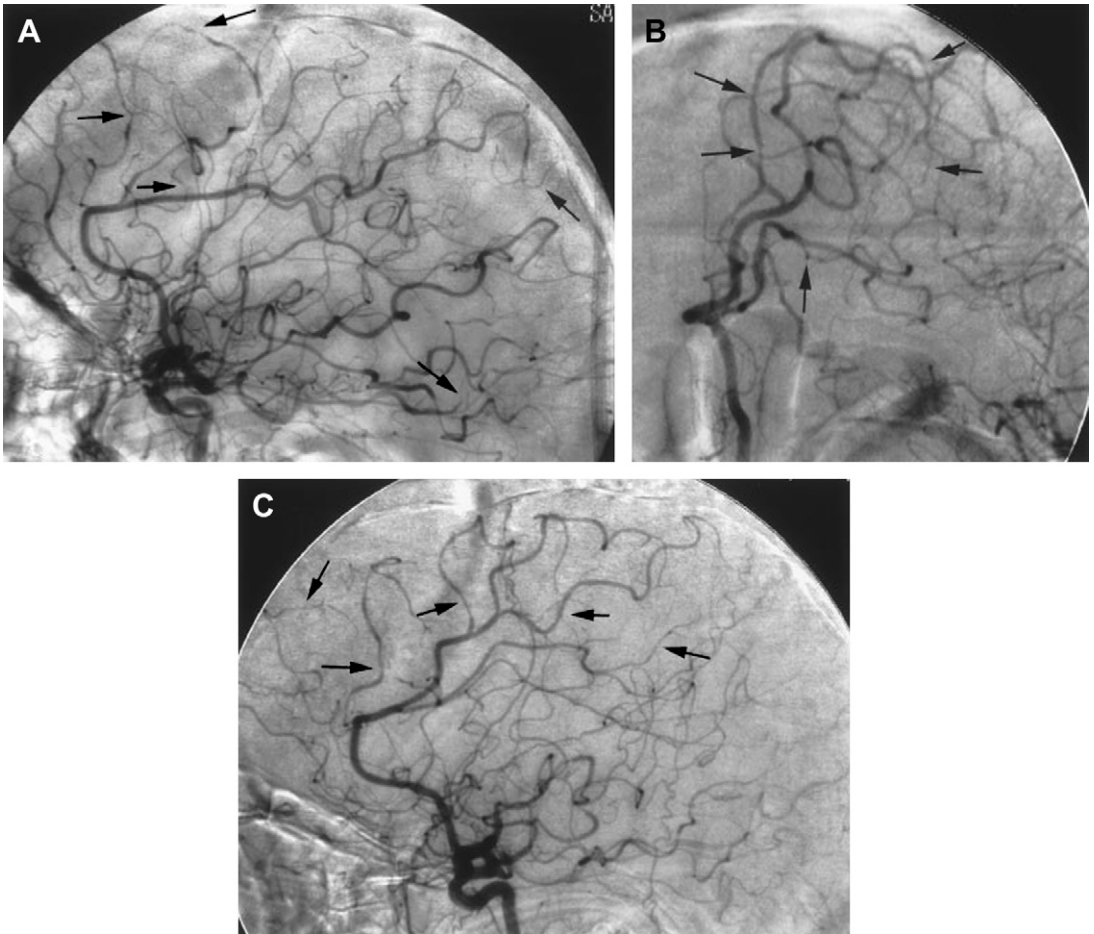


Fig. 11. Varicella zoster virus. Lateral (A) and anteroposterior oblique (B) left internal carotid arteriograms and right internal carotid lateral (C) arteriograms, showing multiple scattered segments (arrows) of irregularity and narrowing involving the small and medium-sized vessels. (From Jain R, Deveikis J, Hickenbottom S, et al. Varicella-zoster vasculitis presenting with intracranial hemorrhage. *AJNR Am J Neuroradiol* 2003;24:972; with permission.)

gray and white matter lesions also seen. Deep and superficial infarcts, some with associated hemorrhage, are seen. Less frequently, VZV vasculopathy results in aneurysm formation, subarachnoid or parenchymal hemorrhage, vascular ectasia, or dissection.⁷³ The treatment for VZV infection is acyclovir.²²

Cytomegalovirus

Cytomegalovirus (CMV) is a ubiquitous herpes virus, which is present in its latent form in the majority of the population. In normal hosts, CMV infection presents with nonspecific clinical manifestations such as febrile illnesses, and the course is usually self limited.⁷⁵ However, reactivation of CMV in an immunocompromised patient can result in disseminated infections, typically of the respiratory system, gastrointestinal system, and occasionally

the CNS. Meningoencephalitis and ventriculitis are the intracranial manifestations (see later discussion). Other neurologic manifestations include retinitis, polyradiculitis, and myelitis, which are not discussed further in this article. Because of the HIV epidemic, CMV encephalitis has emerged as an important clinical entity in adults.⁷⁵ With the introduction of highly active antiretroviral therapy (HAART), there has been a decrease in the prevalence of CMV infection, but familiarity with the entity remains critical.

Imaging findings of CNS infection with CMV include ependymal and subependymal enhancement, which when present is very suspicious for CMV ventriculitis in a patient with AIDS.⁷⁵ Other imaging findings include atrophy and periventricular white matter hyperintensities on T2-weighted/FLAIR imaging. Generalized atrophy is the most commonly reported CT abnormality, but is

a nonspecific finding seen frequently in patients who have AIDS.⁶⁶ Of note, imaging studies may be unremarkable in patients with CMV encephalitis.^{75,76} Rarely CNS infection with CMV may manifest as a ring-enhancing or space-occupying lesion.^{66,76} CMV encephalitis is an important opportunistic infection in HIV-infected and, less frequently, in other immunocompromised individuals.⁷⁵ For CMV encephalitis, combination therapy with intravenous ganciclovir and foscarnet is advocated.^{21,22} However, response of CMV encephalitis and ventriculitis to antiviral drugs is poor.^{21,22,76}

Japanese Encephalitis

Japanese encephalitis (JE) is a flaviviral encephalitis that is a major health problem in Asia, where it is a leading cause of viral encephalitis with 30,000 to 50,000 cases reported annually.⁶⁶ Case fatality rates are reported as up to 60%.⁷⁷ Lesions are typically T2 hyperintense and T1 hypointense on MR imaging, and are seen involving the thalami and brainstem, in particular the substantia nigra, basal ganglia, cerebral cortex, corpus striatum, and cerebellum (Fig. 12).⁷⁷ The most consistent finding in JE is bilateral thalamic lesions with or without hemorrhagic changes on MR imaging.⁶⁶ Handique and colleagues⁷⁷ reported that temporal lobe involvement is present in 17% of patients with JE, but involves the body and tail of the hippocampus and spares the anterior temporal lobe and insula, in contradistinction to HSV-1 encephalitis.

West Nile Virus

West Nile virus (WNV) is a member of the Flaviviridae family that can cause a meningoencephalitis. The WNV appeared in the Western hemisphere in 1999 with an outbreak of encephalitis in the greater New York area.^{78,79} Mosquitoes are the vectors of transmission. Roughly 1 in 150 individuals infected with WNV will develop significant CNS disease, defined as encephalitis, meningitis, or a combination of the two.⁷⁸ Positive MR imaging studies in patients with WNV meningoencephalitis are common though nonspecific. WNV infection should be included in the differential of signal abnormalities involving the deep gray matter, brainstem, or mesial temporal lobes, where it is typically cortical (Fig. 13). Infarcts have also been reported.⁷⁸ Of note, MR studies may be normal in patients with WNV encephalitis. Flaccid paralysis has been reported in multiple cases of WNV, and spine MR findings include anterior horn signal abnormalities and enhancement of the cauda equina.⁷⁸

Rabies

Rabies encephalitis is a rare acute infection of the CNS by caused by an RNA virus of the rhabdovirus family. The mode of transmission to humans is primarily via the bites of rabid animals. After inoculation the virus reaches the CNS through retrograde axoplasmic flow.⁸⁰ Human rabies presents in two forms: encephalitic and paralytic. In the CNS there is an initial proclivity toward infection

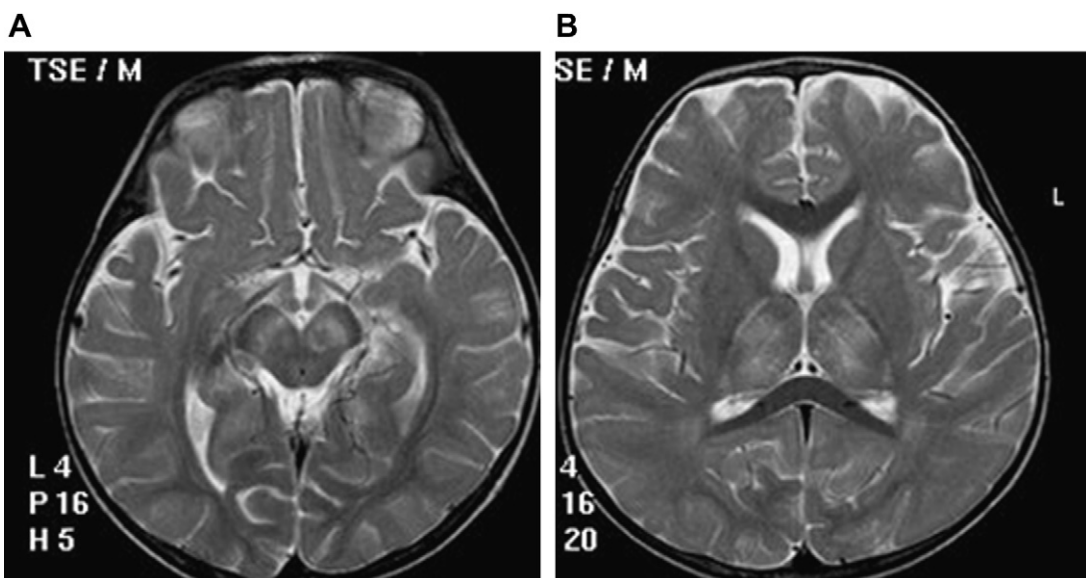


Fig. 12. Japanese encephalitis. (A, B) T2-weighted image demonstrates abnormal signal involving the midbrain (A) and bilateral thalami (B). (Courtesy of Hemant Parmar, MD, University of Michigan.)

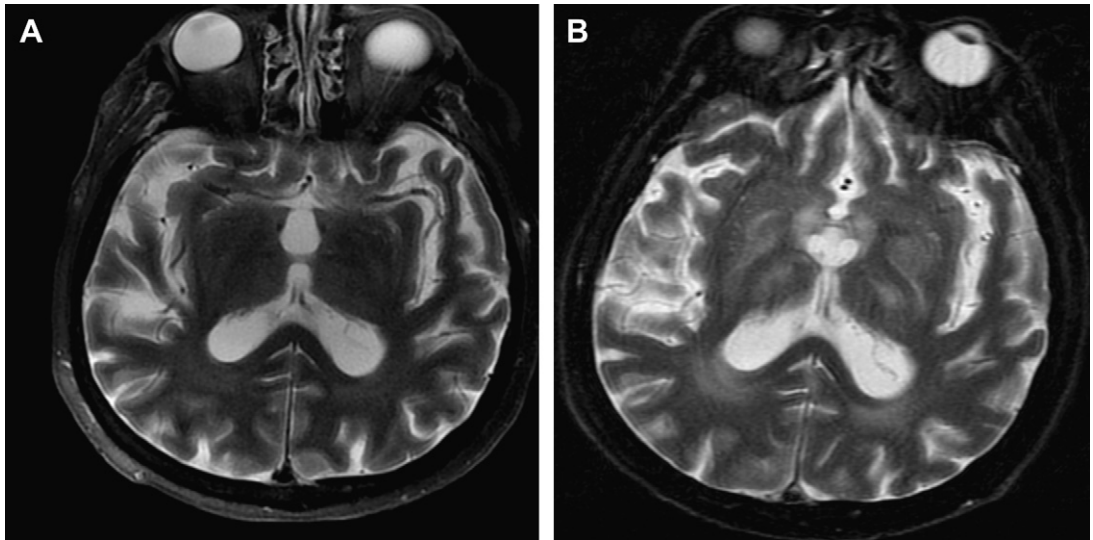


Fig. 13. West Nile virus. (A) T2-weighted images are initially unremarkable other than for age-related volume loss. (B) T2-weighted image acquired 2 months later demonstrates abnormal T2 signal involving the thalami and imaged portions of the inferior basal ganglia bilaterally.

of the gray matter. Reports of imaging findings in patients infected with the rabies virus are sparse. Reported imaging findings include areas of hypoattenuation on CT and hyperintensity on T2-weighted imaging involving the brainstem, basal ganglia, and thalamus (**Fig. 14**).^{80,81} An abnormal signal on the T2-weighted image involving the hippocampi, cerebral white matter, and central gray matter of the cord can also be seen.⁶⁶ Associated mild to moderate enhancement of these lesions is a late feature.⁸⁰ The imaging findings can support the diagnosis of rabies encephalitis in the appropriate clinical context.

Subacute Encephalitis

Subacute encephalitis refers to cases in which the onset of symptoms is insidious when compared with the clinical course of acute encephalitis, examples of which are discussed earlier in this article. Many infections fall into this category. Some disease processes that radiologists should be aware of include HIV encephalitis (HIVE), progressive multifocal leukoencephalopathy (PML), cytomegalovirus encephalitis, which can result in either acute or chronic encephalitis, Creutzfeldt-Jakob disease (CJD), and subacute sclerosing panencephalitis.

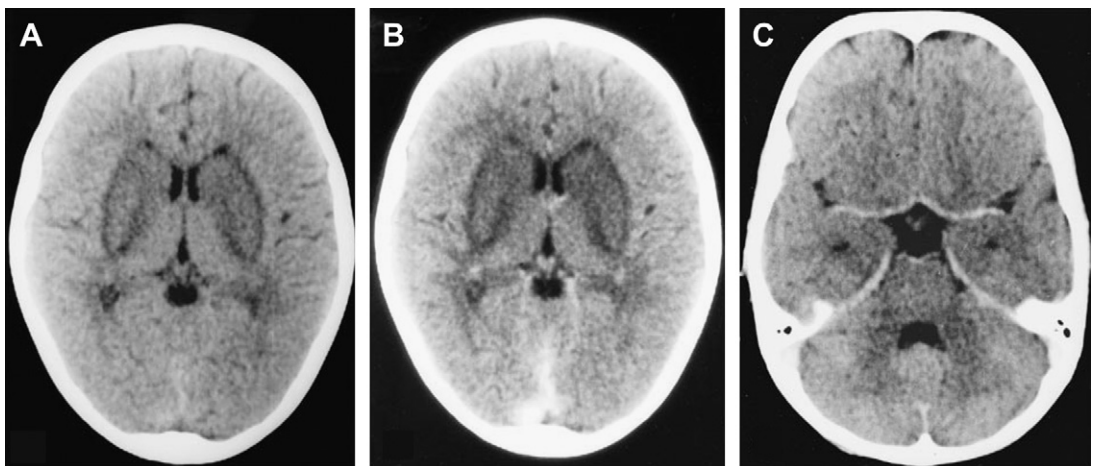


Fig. 14. Rabies. (A–C) Noncontrast (A) and contrast-enhanced (B, C) CT scans show nonenhancing bilateral basal ganglia hypodensities. (From Awasthi M, Parmar H, Patankar T, et al. Imaging findings in rabies encephalitis. *AJNR Am J Neuroradiol* 2001;22:678; with permission.)

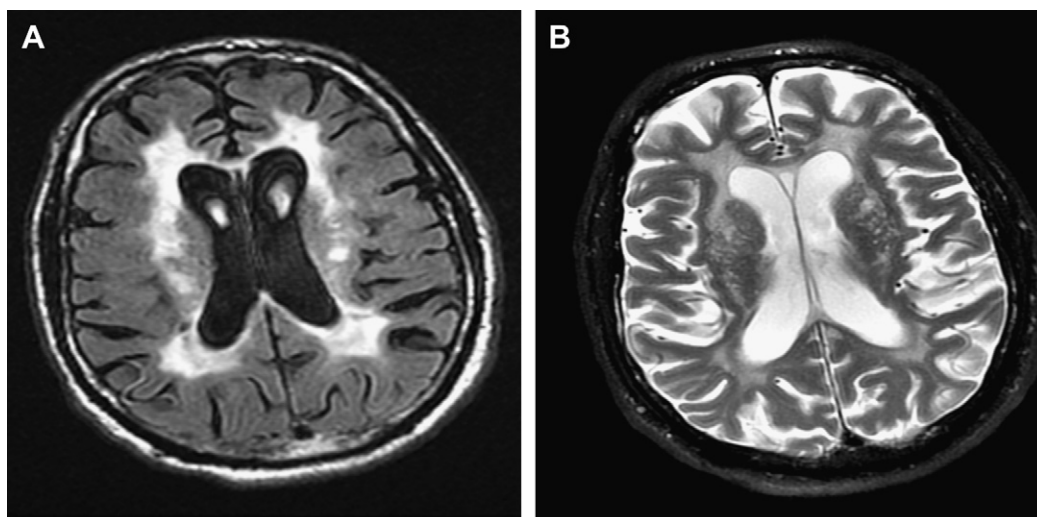


Fig. 15. Human immunodeficiency virus encephalitis. FLAIR (A) and T2-weighted (B) MR images demonstrate volume loss and periventricular and deep white matter signal abnormality without mass effect.

HIV Encephalitis

AIDS dementia complex is a syndrome of cognitive, behavioral, and motor abnormalities attributed to direct HIV infection of the brain. The imaging findings of AIDS dementia complex are frequently referred to as HIVE.⁷⁶ The typical imaging appearance is the combination of atrophy and periventricular, relatively symmetric areas of T2 signal abnormality. HIVE does not result in mass effect or enhancement. If either of these findings is present, another diagnosis must be considered (**Fig. 15**). Proton ¹H-NMR spectroscopy reveals decreased NAA and elevated peaks of choline and myo-inositol.⁸² Magnetization transfer ratios (MTR) are reported to help differentiate HIVE from PML. There is a marked decrease in MTR with PML lesions, thought to be secondary to demyelination.⁸³ DTI has been reported to depict abnormalities in mean diffusivity and fractional anisotropy in the subcortical white matter, even when the brain appears normal on conventional MR images in HIV-positive patients. Of note, the patients in whom statistically significant differences were noted were those not receiving HAART and with detectable viral loads.⁸⁴ Other investigators have found DTI to be not fully helpful in identifying patients with early HIV infection.⁸⁵ The clinical role of imaging with DTI in HIV patients seems to be relatively limited at this point. Nonetheless, imaging plays a crucial role in the management and evaluation for infections in HIV patients.

Progressive Multifocal Leukoencephalopathy

PML results from infection of the oligodendrocytes with a papovavirus, JC virus, named after the index patient.⁸⁶ PML is most commonly seen in patients

with AIDS, but can occur in a spectrum of immunocompromised patients. PML results in progressive neurologic decline. The JC virus directly infects the oligodendrocytes, which are thus unable to maintain myelin. The resultant white matter lesions are typically multiple, bilateral, asymmetric, and confluent.⁸⁶ Any region of the brain may be infected, but there is some increased prevalence of lesions seen in the parietal lobe, and overall supratentorial lesions predominate over infratentorial lesions.⁸⁶ The lesions demonstrate increased T2 and decreased T1 signal, and corresponding low attenuation on CT images (**Figs. 16** and **17**).

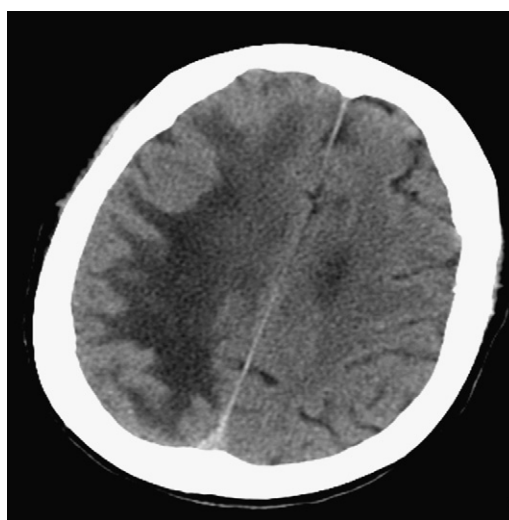


Fig. 16. Progressive multifocal leukoencephalopathy (PML). Noncontrast head CT demonstrates extensive abnormal low attenuation within the right frontal and parietal lobes.

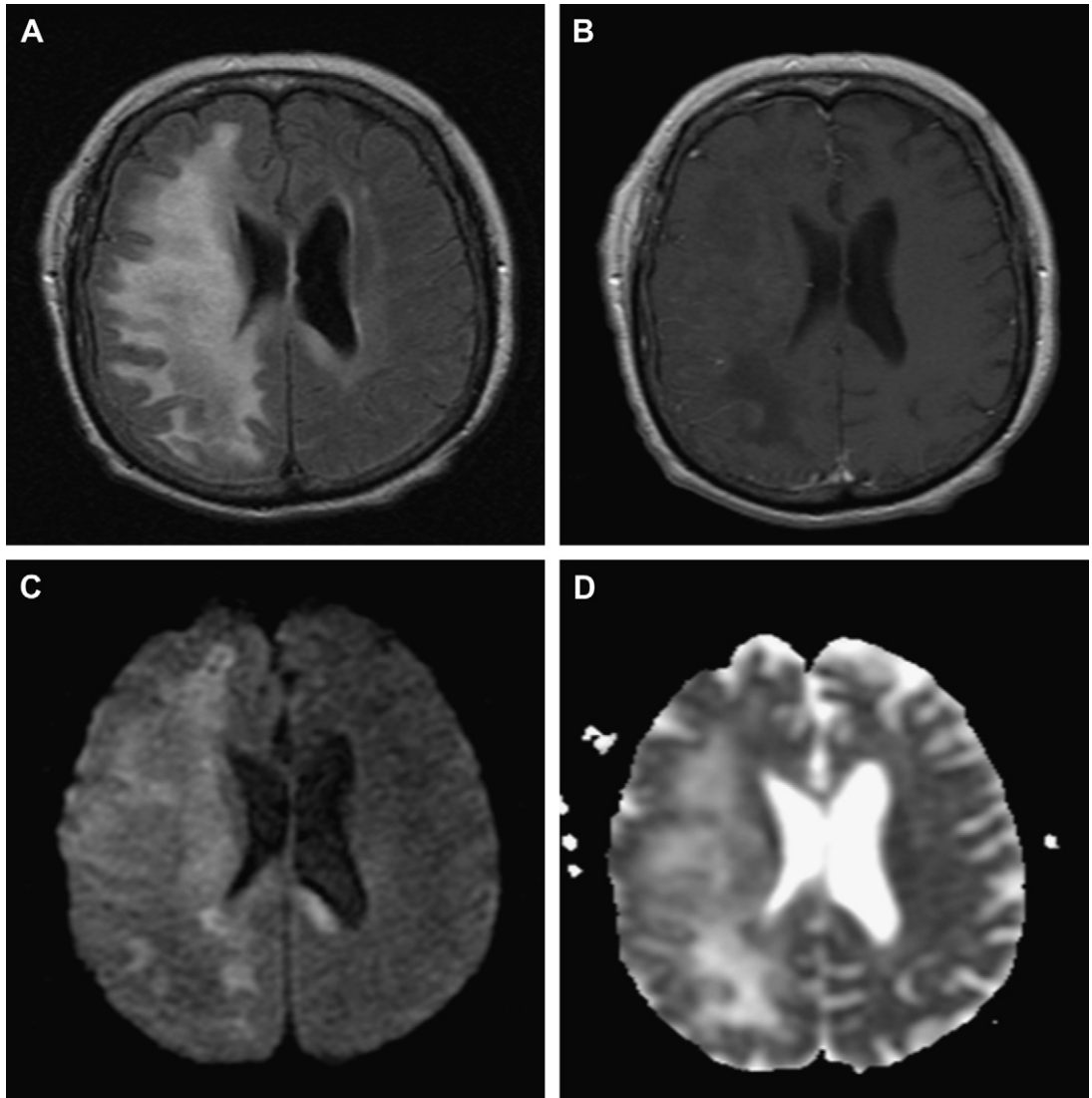


Fig. 17. PML. MR imaging FLAIR (A), T1 postcontrast (B), diffusion-weighted, (C), and ADC map (D) images. (A) Extensive right hemispheric white matter and subtle left periventricular signal abnormality is noted, with some mass effect in the form of flattening of the right lateral ventricle. (B) Minimal associated enhancement is appreciated. (C, D) Scattered areas of peripheral restricted diffusion are noted with corresponding decreased signal on the ADC maps.

Significant mass effect or enhancement is uncommon; although peripheral enhancement has been reported.^{76,86} A key point to remember is that PML typically involves the peripheral white matter, involving the subcortical U fibers,⁸⁷ whereas CMV and HIV tend to involve the periventricular white matter. Furthermore, in patients with PML the CT and MR findings discussed earlier are typically asymmetric compared with the more symmetric abnormalities noted with HIV.⁷⁶ The degree of brain atrophy is significantly milder in PML than that seen in HIV,⁸⁶ although considerable overlap of these disease processes exists.⁷⁶

PML lesions can demonstrate patchy restricted diffusion that is frequently peripheral and is thought to correlate with areas of lesion expansion.^{87,88}

There is some evidence that diffusion-weighted images can evaluate for response of PML to HAART. Specifically, Usiskin and colleagues⁸⁹ described PML lesions demonstrating marked reduction in lesional ADC and reconstitution of anisotropy in the affected areas that correlated with treatment response, although this was a case report (see Fig. 17). Some early research also suggests that patients with rapid clinical progression following initiation of HAART have lesions with higher ADC

values and are at risk of developing immune reconstitution inflammatory syndrome.⁸⁸ MR spectroscopic analysis of the affected white matter may demonstrate decreased NAA, elevated choline, presence of lactate, increased lipids, and potential elevation in *myo*-inositol levels.⁹⁰ Again, MTR are reported to help differentiate HIV and PML. There is a marked decrease in MTR with PML lesions, thought to be secondary to demyelination.⁸³

Creutzfeldt-Jakob Disease

CJD is a spongiform encephalopathy characterized by progressive dementia. The infecting organism is a prion. CJD is classified into sporadic CJD, familial CJD, and acquired forms. The

so-called acquired forms include new variant CJD, kuru, and iatrogenic CJD. New variant CJD has similarities to bovine spongiform encephalopathy, which is thought to be transmitted from infected cattle to humans. Kuru was first described in brain-eating cannibals in New Guinea.⁹¹ Iatrogenic CJD has been described in patients following corneal transplants, ingestion of prior contaminated human growth hormone, and following transplantation of cadaveric dural matter.⁹¹ Approximately 85% of the cases are classified as sporadic CJD with an unknown source of infection.⁶⁶ Hereditary CJD accounts for approximately 10% of cases. Rapidly progressive dementia, periodic synchronous discharges on the electroencephalogram, and myoclonus are classic

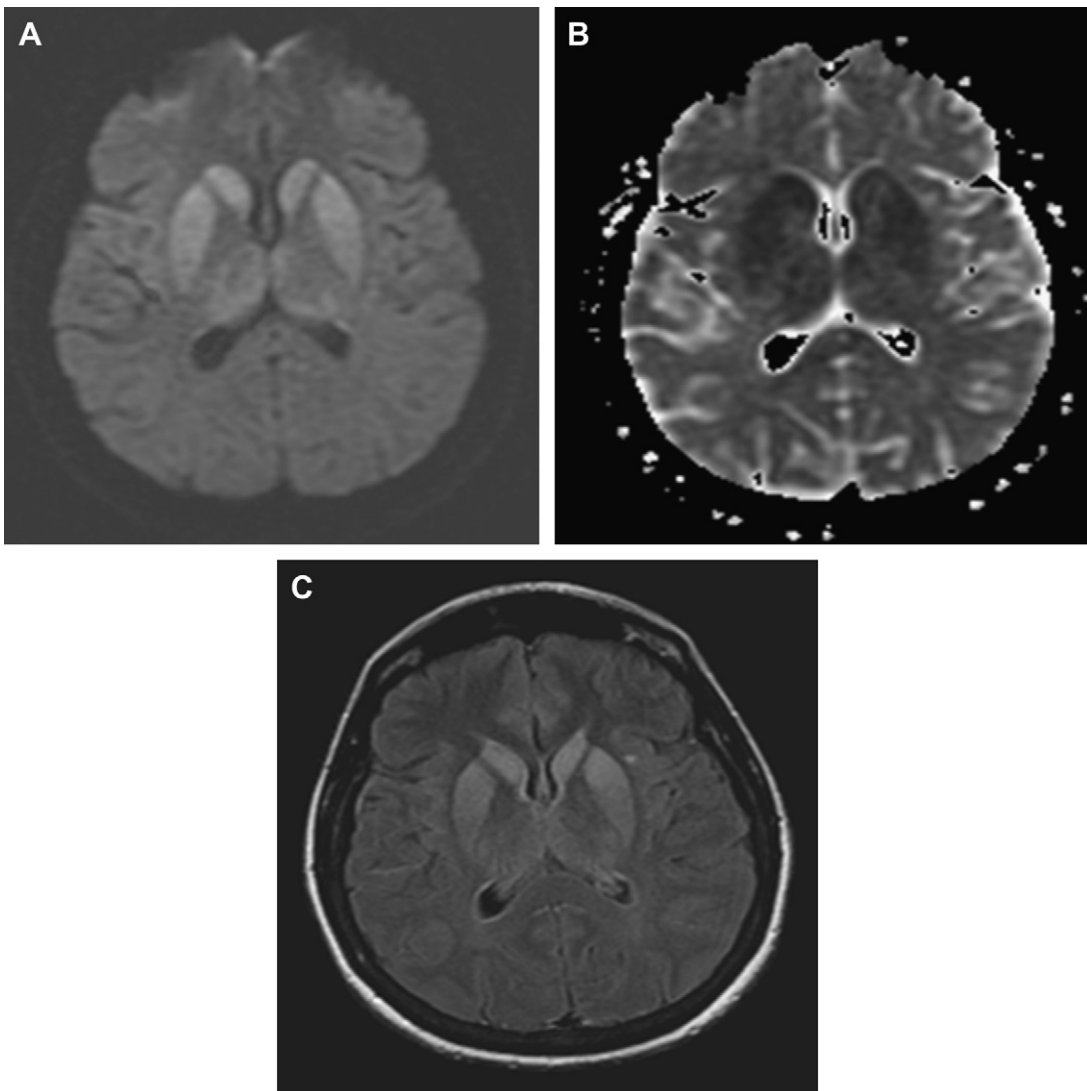


Fig. 18. Creutzfeldt-Jakob disease. MR diffusion-weighted (A), ADC map (B), and FLAIR (C) images. True restricted diffusion involving the basal ganglia and thalamus (pulvinar) are noted.

features of sporadic CJD. Typical MR imaging findings in sporadic CJD are areas of restricted diffusion along the cortex and involving the deep gray matter structures; corresponding hyperintensity on the T2-weighted and FLAIR sequences can be seen.⁷⁴ The characteristic MR imaging abnormality in new variant CJD is restricted diffusion and hyperintensity on T2-weighted imaging involving the pulvinar nuclei (**Fig. 18**).⁹²

SUMMARY

CT and MR imaging have had a great impact on the diagnosis and management of brain abscess. CT provides a rapid means of localization, guidance for stereotactic aspiration, and serial postoperative evaluation. MR imaging has improved sensitivity for the detection of cerebral abscess and its associated complications. Restricted diffusion within a ring-enhancing mass is typical but not pathognomonic of a brain abscess. In cases of uncertainty, MR spectroscopy complements diffusion-weighted imaging and can improve diagnostic confidence. Abscess drainage with targeted antimicrobial therapy remains the standard treatment.

The cause of encephalitis can be suggested in some cases based on imaging findings, particularly when combined with CSF and serologic studies and patient history including age, immune status, and geographic and seasonal information.

REFERENCES

- Smirniotopoulos JG, Murphy FM, Rushing EJ, et al. Patterns of contrast enhancement in the brain and meninges. *Radiographics* 2007;27(2):525–51.
- Mamelak AN, Mampalam TJ, Obana WG, et al. Improved management of multiple brain abscesses: a combined surgical and medical approach. *Neurosurgery* 1995;36(1):76–85 [discussion: 6].
- Mathisen GE, Johnson JP. Brain abscess. *Clin Infect Dis* 1997;25(4):763–79 [quiz: 80–1].
- Macewen W. Pyogenic infective disease of the brain and spinal cord. Meningitis, abscess of the brain and infective sinus thrombosis. Glasgow (United Kingdom): James Maclehose and Sons; 1893.
- Canale DJ. William Macewen and the treatment of brain abscesses: revisited after one hundred years. *J Neurosurg* 1996;84(1):133–42.
- Cavusoglu H, Kaya RA, Turkmenoglu ON, et al. Brain abscess: analysis of results in a series of 51 patients with a combined surgical and medical approach during an 11-year period. *Neurosurg Focus* 2008;24(6):E9.
- Brewer NS, MacCarty CS, Wellman WE. Brain abscess: a review of recent experience. *Ann Intern Med* 1975;82(4):571–6.
- Carey ME, Chou SN, French LA. Experience with brain abscesses. *J Neurosurg* 1972;36(1):1–9.
- Carpenter J, Stapleton S, Holliman R. Retrospective analysis of 49 cases of brain abscess and review of the literature. *Eur J Clin Microbiol Infect Dis* 2007;26(1):1–11.
- Garfield J. Management of supratentorial intracranial abscess: a review of 200 cases. *Br Med J* 1969;2(5648):7–11.
- Hakan T, Ceran N, Erdem I, et al. Bacterial brain abscesses: an evaluation of 96 cases. *J Infect* 2006;52(5):359–66.
- Menon S, Bharadwaj R, Chowdhary A, et al. Current epidemiology of intracranial abscesses: a prospective 5 year study. *J Med Microbiol* 2008;57(Pt 10):1259–68.
- Sharma R, Mohandas K, Cooke RP. Intracranial abscesses: changes in epidemiology and management over five decades in Merseyside. *Infection* 2009;37(1):39–43.
- Xiao F, Tseng MY, Teng LJ, et al. Brain abscess: clinical experience and analysis of prognostic factors. *Surg Neurol* 2005;63(5):442–9 [discussion: 9–50].
- Alderson D, Strong AJ, Ingham HR, et al. Fifteen-year review of the mortality of brain abscess. *Neurosurgery* 1981;8(1):1–6.
- de Louvois J. Bacteriological examination of pus from abscesses of the central nervous system. *J Clin Pathol* 1980;33(1):66–71.
- Miller ES, Dias PS, Uttley D. CT scanning in the management of intracranial abscess: a review of 100 cases. *Br J Neurosurg* 1988;2(4):439–46.
- Rosenblum ML, Hoff JT, Norman D, et al. Decreased mortality from brain abscesses since advent of computerized tomography. *J Neurosurg* 1978;49(5):658–68.
- Walsh PR, Larson SJ, Rytel MW, et al. Stereotactic aspiration of deep cerebral abscesses after CT-directed labeling. *Appl Neurophysiol* 1980;43(3–5):205–9.
- Wise BL, Gleason CA. CT-directed stereotactic surgery in the management of brain abscess. *Ann Neurol* 1979;6(5):457.
- Kennedy PG. Viral encephalitis: causes, differential diagnosis, and management. *J Neurol Neurosurg Psychiatry* 2004;75(Suppl 1):i10–5.
- Steiner I, Budka H, Chaudhuri A, et al. Viral meningoencephalitis: a review of diagnostic methods and guidelines for management. *Eur J Neurol* 2010;17(8):999. e57.
- Friedlander RM, Gonzalez RG, Afridi NA, et al. Case records of the Massachusetts General Hospital. Weekly clinicopathological exercises. Case 16-2003. A 58-year-old woman with left-sided weakness and a right frontal brain mass. *N Engl J Med* 2003;348(21):2125–32.
- Saez-Llorens XJ, Umana MA, Odio CM, et al. Brain abscess in infants and children. *Pediatr Infect Dis J* 1989;8(7):449–58.

25. Lu CH, Chang WN, Lin YC, et al. Bacterial brain abscess: microbiological features, epidemiological trends and therapeutic outcomes. *QJM* 2002;95(8): 501–9.
26. Prasad KN, Mishra AM, Gupta D, et al. Analysis of microbial etiology and mortality in patients with brain abscess. *J Infect* 2006;53(4):221–7.
27. Yang KY, Chang WN, Ho JT, et al. Postneurosurgical nosocomial bacterial brain abscess in adults. *Infection* 2006;34(5):247–51.
28. Mamelak AN, Obana WG, Flaherty JF, et al. Nocardial brain abscess: treatment strategies and factors influencing outcome. *Neurosurgery* 1994;35(4):622–31.
29. Britt RH, Enzmann DR. Clinical stages of human brain abscesses on serial CT scans after contrast infusion. Computerized tomographic, neuropathological, and clinical correlations. *J Neurosurg* 1983;59(6):972–89.
30. Haines AB, Zimmerman RD, Morgello S, et al. MR imaging of brain abscesses. *AJR Am J Roentgenol* 1989;152(5):1073–85.
31. Baldwin AC, Kielian T. Persistent immune activation associated with a mouse model of *Staphylococcus aureus*-induced experimental brain abscess. *J Neuroimmunol* 2004;151(1–2):24–32.
32. Enzmann DR, Britt RH, Yeager AS. Experimental brain abscess evolution: computed tomographic and neuropathologic correlation. *Radiology* 1979; 133(1):113–22.
33. Yuh WT, Nguyen HD, Gao F, et al. Brain parenchymal infection in bone marrow transplantation patients: CT and MR findings. *AJR Am J Roentgenol* 1994;162(2):425–30.
34. Seydoux C, Francioli P. Bacterial brain abscesses: factors influencing mortality and sequelae. *Clin Infect Dis* 1992;15(3):394–401.
35. Desprechins B, Stadnik T, Koerts G, et al. Use of diffusion-weighted MR imaging in differential diagnosis between intracerebral necrotic tumors and cerebral abscesses. *AJNR Am J Neuroradiol* 1999; 20(7):1252–7.
36. Kita T, Hayashi K, Yamamoto M, et al. Does supplementation of contrast MR imaging with thallium-201 brain SPECT improve differentiation between benign and malignant ring-like contrast-enhanced cerebral lesions? *Ann Nucl Med* 2007;21(5):251–6.
37. Martinez del Valle MD, Gomez-Rio M, Horcajadas A, et al. False positive thallium-201 SPECT imaging in brain abscess. *Br J Radiol* 2000;73(866):160–4.
38. Skiest DJ. Focal neurological disease in patients with acquired immunodeficiency syndrome. *Clin Infect Dis* 2002;34(1):103–15.
39. Ebisu T, Tanaka C, Umeda M, et al. Discrimination of brain abscess from necrotic or cystic tumors by diffusion-weighted echo planar imaging. *Magn Reson Imaging* 1996;14(9):1113–6.
40. Kim YJ, Chang KH, Song IC, et al. Brain abscess and necrotic or cystic brain tumor: discrimination with signal intensity on diffusion-weighted MR imaging. *AJR Am J Roentgenol* 1998;171(6):1487–90.
41. Lai PH, Ho JT, Chen WL, et al. Brain abscess and necrotic brain tumor: discrimination with proton MR spectroscopy and diffusion-weighted imaging. *AJNR Am J Neuroradiol* 2002;23(8):1369–77.
42. Noguchi K, Watanabe N, Nagayoshi T, et al. Role of diffusion-weighted echo-planar MRI in distinguishing between brain abscess and tumour: a preliminary report. *Neuroradiology* 1999;41(3):171–4.
43. Mishra AM, Gupta RK, Saksena S, et al. Biological correlates of diffusivity in brain abscess. *Magn Reson Med* 2005;54(4):878–85.
44. Cartes-Zumelzu FW, Stavrou I, Castillo M, et al. Diffusion-weighted imaging in the assessment of brain abscesses therapy. *AJNR Am J Neuroradiol* 2004;25(8):1310–7.
45. Fanning NF, Laffan EE, Shroff MM. Serial diffusion-weighted MRI correlates with clinical course and treatment response in children with intracranial pus collections. *Pediatr Radiol* 2006;36(1):26–37.
46. Park SH, Chang KH, Song IC, et al. Diffusion-weighted MRI in cystic or necrotic intracranial lesions. *Neuroradiology* 2000;42(10):716–21.
47. Holtas S, Geijer B, Stromblad LG, et al. A ring-enhancing metastasis with central high signal on diffusion-weighted imaging and low apparent diffusion coefficients. *Neuroradiology* 2000;42(11):824–7.
48. Lai PH, Hsu SS, Ding SW, et al. Proton magnetic resonance spectroscopy and diffusion-weighted imaging in intracranial cystic mass lesions. *Surg Neurol* 2007;68(Suppl 1):S25–36.
49. Tung GA, Evangelista P, Rogg JM, et al. Diffusion-weighted MR imaging of rim-enhancing brain masses: is markedly decreased water diffusion specific for brain abscess? *AJR Am J Roentgenol* 2001;177(3):709–12.
50. Mishra AM, Gupta RK, Jaggi RS, et al. Role of diffusion-weighted imaging and in vivo proton magnetic resonance spectroscopy in the differential diagnosis of ring-enhancing intracranial cystic mass lesions. *J Comput Assist Tomogr* 2004; 28(4):540–7.
51. Nath K, Agarwal M, Ramola M, et al. Role of diffusion tensor imaging metrics and in vivo proton magnetic resonance spectroscopy in the differential diagnosis of cystic intracranial mass lesions. *Magn Reson Imaging* 2009;27(2):198–206.
52. Kim SH, Chang KH, Song IC, et al. Brain abscess and brain tumor: discrimination with in vivo H-1 MR spectroscopy. *Radiology* 1997;204(1):239–45.
53. Lai PH, Li KT, Hsu SS, et al. Pyogenic brain abscess: findings from in vivo 1.5-T and 11.7-T in vitro proton MR spectroscopy. *AJNR Am J Neuroradiol* 2005; 26(2):279–88.
54. Pal D, Bhattacharyya A, Husain M, et al. In vivo proton MR spectroscopy evaluation of pyogenic

- brain abscesses: a report of 194 cases. *AJNR Am J Neuroradiol* 2010;31(2):360–6.
55. Grand S, Passaro G, Ziegler A, et al. Necrotic tumor versus brain abscess: importance of amino acids detected at 1H MR spectroscopy—initial results. *Radiology* 1999;213(3):785–93.
 56. Garg M, Gupta RK, Husain M, et al. Brain abscesses: etiologic categorization with in vivo proton MR spectroscopy. *Radiology* 2004;230(2):519–27.
 57. Burtscher IM, Holtas S. In vivo proton MR spectroscopy of untreated and treated brain abscesses. *AJNR Am J Neuroradiol* 1999;20(6):1049–53.
 58. Chiang IC, Hsieh TJ, Chiu ML, et al. Distinction between pyogenic brain abscess and necrotic brain tumour using 3-tesla MR spectroscopy, diffusion and perfusion imaging. *Br J Radiol* 2009;82(982):813–20.
 59. Chan JH, Tsui EY, Chau LF, et al. Discrimination of an infected brain tumor from a cerebral abscess by combined MR perfusion and diffusion imaging. *Comput Med Imaging Graph* 2002;26(1):19–23.
 60. Gupta RK, Hasan KM, Mishra AM, et al. High fractional anisotropy in brain abscesses versus other cystic intracranial lesions. *AJNR Am J Neuroradiol* 2005;26(5):1107–14.
 61. Gupta RK, Nath K, Prasad A, et al. In vivo demonstration of neuroinflammatory molecule expression in brain abscess with diffusion tensor imaging. *AJNR Am J Neuroradiol* 2008;29(2):326–32.
 62. Nath K, Ramola M, Husain M, et al. Assessment of therapeutic response in patients with brain abscess using diffusion tensor imaging. *World Neurosurg* 2010;73(1):63–8 [discussion: e6].
 63. Mampalam TJ, Rosenblum ML. Trends in the management of bacterial brain abscesses: a review of 102 cases over 17 years. *Neurosurgery* 1988;23(4):451–8.
 64. Tattevin P, Bruneel F, Clair B, et al. Bacterial brain abscesses: a retrospective study of 94 patients admitted to an intensive care unit (1980 to 1999). *Am J Med* 2003;115(2):143–6.
 65. Zeidman SM, Geisler FH, Olivi A. Intraventricular rupture of a purulent brain abscess: case report. *Neurosurgery* 1995;36(1):189–93 [discussion: 93].
 66. Tali ET. Viruses and prion in the CNS. Preface. *Neuroimaging Clin N Am* 2008;18(1):xiii–xxiv.
 67. Baringer JR. Herpes simplex infections of the nervous system. *Neurol Clin* 2008;26(3):657–74, viii.
 68. Falcone S, Post MJ. Encephalitis, cerebritis, and brain abscess: pathophysiology and imaging findings. *Neuroimaging Clin N Am* 2000;10(2):333–53.
 69. Noguchi T, Yoshiura T, Hiwatashi A, et al. CT and MRI findings of human herpesvirus 6-associated encephalopathy: comparison with findings of herpes simplex virus encephalitis. *AJR Am J Roentgenol* 2010;194(3):754–60.
 70. Foerster BR, Thurnher MM, Malani PN, et al. Intracranial infections: clinical and imaging characteristics. *Acta Radiol* 2007;48(8):875–93.
 71. Menon DK, Sargentoni J, Peden CJ, et al. Proton MR spectroscopy in herpes simplex encephalitis: assessment of neuronal loss. *J Comput Assist Tomogr* 1990;14(3):449–52.
 72. Samann PG, Schlegel J, Muller G, et al. Serial proton MR spectroscopy and diffusion imaging findings in HIV-related herpes simplex encephalitis. *AJNR Am J Neuroradiol* 2003;24(10):2015–9.
 73. Gilden D, Cohrs RJ, Mahalingam R, et al. Varicella zoster virus vasculopathies: diverse clinical manifestations, laboratory features, pathogenesis, and treatment. *Lancet Neurol* 2009;8(8):731–40.
 74. Katchanov J, Siebert E, Klingebiel R, et al. Infectious vasculopathy of intracranial large- and medium-sized vessels in neurological intensive care unit: a clinico-radiological study. *Neurocrit Care* 2010;12(3):369–74.
 75. Arribas JR, Storch GA, Clifford DB, et al. Cytomegalovirus encephalitis. *Ann Intern Med* 1996;125(7):577–87.
 76. Smith AB, Smirniotopoulos JG, Rushing EJ. From the archives of the AFIP: central nervous system infections associated with human immunodeficiency virus infection: radiologic-pathologic correlation. *Radiographics* 2008;28(7):2033–58.
 77. Handique SK, Das RR, Barman K, et al. Temporal lobe involvement in Japanese encephalitis: problems in differential diagnosis. *AJNR Am J Neuroradiol* 2006;27(5):1027–31.
 78. Petropoulou KA, Gordon SM, Prayson RA, et al. West Nile virus meningoencephalitis: MR imaging findings. *AJNR Am J Neuroradiol* 2005;26(8):1986–95.
 79. Asnis DS, Conetta R, Teixeira AA, et al. The West Nile Virus outbreak of 1999 in New York: the Flushing Hospital experience. *Clin Infect Dis* 2000;30(3):413–8.
 80. Laothamatas J, Hemachudha T, Mitrabhakdi E, et al. MR imaging in human rabies. *AJNR Am J Neuroradiol* 2003;24(6):1102–9.
 81. Awasthi M, Parmar H, Patankar T, et al. Imaging findings in rabies encephalitis. *AJNR Am J Neuroradiol* 2001;22(4):677–80.
 82. Laubenberger J, Haussinger D, Bayer S, et al. HIV-related metabolic abnormalities in the brain: depiction with proton MR spectroscopy with short echo times. *Radiology* 1996;199(3):805–10.
 83. Ernst T, Chang L, Witt M, et al. Progressive multifocal leukoencephalopathy and human immunodeficiency virus-associated white matter lesions in AIDS: magnetization transfer MR imaging. *Radiology* 1999;210(2):539–43.

84. Filippi CG, Ulug AM, Ryan E, et al. Diffusion tensor imaging of patients with HIV and normal-appearing white matter on MR images of the brain. *AJNR Am J Neuroradiol* 2001;22(2):277–83.
85. Thurnher MM, Castillo M, Stadler A, et al. Diffusion-tensor MR imaging of the brain in human immunodeficiency virus-positive patients. *AJNR Am J Neuroradiol* 2005;26(9):2275–81.
86. Post MJ, Yiannoutsos C, Simpson D, et al. Progressive multifocal leukoencephalopathy in AIDS: are there any MR findings useful to patient management and predictive of patient survival? AIDS Clinical Trials Group, 243 Team. *AJNR Am J Neuroradiol* 1999;20(10):1896–906.
87. Kuker W, Mader I, Nagele T, et al. Progressive multifocal leukoencephalopathy: value of diffusion-weighted and contrast-enhanced magnetic resonance imaging for diagnosis and treatment control. *Eur J Neurol* 2006;13(8):819–26.
88. Buckle C, Castillo M. Use of diffusion-weighted imaging to evaluate the initial response of progressive multifocal leukoencephalopathy to highly active antiretroviral therapy: early experience. *AJNR Am J Neuroradiol* 2010;31(6):1031–5.
89. Usiskin SI, Bainbridge A, Miller RF, et al. Progressive multifocal leukoencephalopathy: serial high-b-value diffusion-weighted MR imaging and apparent diffusion coefficient measurements to assess response to highly active antiretroviral therapy. *AJNR Am J Neuroradiol* 2007;28(2):285–6.
90. Chang L, Ernst T, Tornatore C, et al. Metabolite abnormalities in progressive multifocal leukoencephalopathy by proton magnetic resonance spectroscopy. *Neurology* 1997;48(4):836–45.
91. Ukisu R, Kushihashi T, Tanaka E, et al. Diffusion-weighted MR imaging of early-stage Creutzfeldt-Jakob disease: typical and atypical manifestations. *Radiographics* 2006;26(Suppl 1):S191–204.
92. Zeidler M, Sellar RJ, Collie DA, et al. The pulvinal sign on magnetic resonance imaging in variant Creutzfeldt-Jakob disease. *Lancet* 2000;355(9213):1412–8.